AD-A191 649 QUANTITATIVE USE OF EXCIPLEX-BASED VAPOR/LIQUID VISUALIZATION SYSTEMS (USERS MANUAL)(U) TEXAS UNIV AT DALLAS RICHARDSON L A MELTON 14 JAN 88 ARO-24060.2-EG 1/1

UNCLASSIFIED DAAL-86-K-0002 F/G 21/2 NL

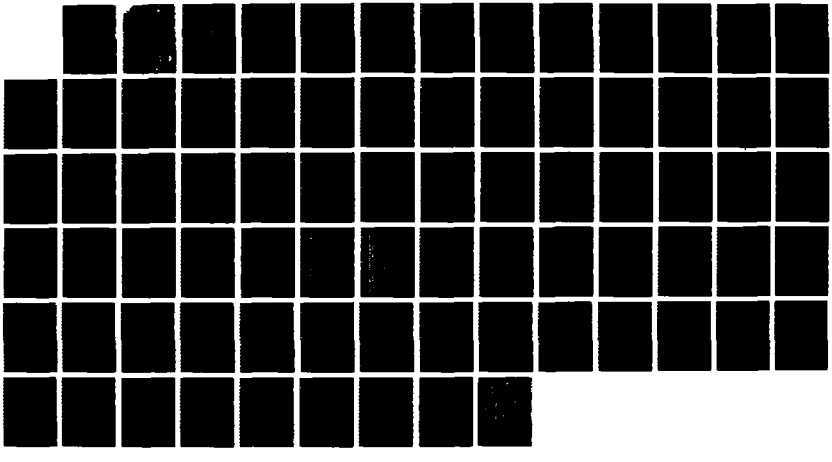

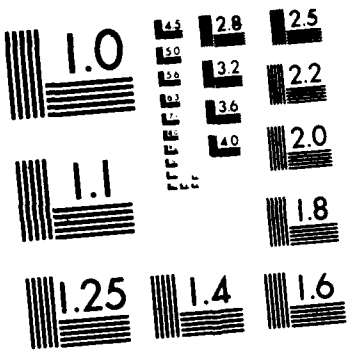

QUANTITATIVE USE OF EXCIPLEX-BASED VAPOR/LIQUID VISUALIZATION SYSTEMS (A USERS MANUAL)

FINAL REPORT

LYNN A. MELTON

JANUARY 1, 1988

U. S. ARMY RESEARCH OFFICE

CONTRACT DAAL03-86-K-0082

UNIVERSITY OF TEXAS AT DALLAS
P.O. BOX 830688
RICHARDSON, TEXAS 75083

UNCLASSIFIED

SECURITY CLASSIFICATION OF THIS PAGE

REPORT DOCUMENTATION PAGE

1a. REPORT SECURITY CLASSIFICATION Unclassified	1b. RESTRICTIVE MARKINGS
2a. SECURITY CLASSIFICATION AUTHORITY	3. DISTRIBUTION/AVAILABILITY OF REPORT Approved for public release; distribution unlimited.
2b. DECLASSIFICATION/DOWNGRADING SCHEDULE	
4. PERFORMING ORGANIZATION REPORT NUMBER(S)	5. MONITORING ORGANIZATION REPORT NUMBER(S) ARO 24068.2-EG
6a. NAME OF PERFORMING ORGANIZATION University of Texas at Dallas 6b. OFFICE SYMBOL (If applicable)	7a. NAME OF MONITORING ORGANIZATION U. S. Army Research Office
6c. ADDRESS (City, State, and ZIP Code) Office of Sponsored Projects P.O. Box 830688 Richardson, TX 75083-0688	7b. ADDRESS (City, State, and ZIP Code) P. O. Box 12211 Research Triangle Park, NC 27709-2211
8a. NAME OF FUNDING/SPONSORING ORGANIZATION U. S. Army Research Office 8b. OFFICE SYMBOL (If applicable)	9. PROCUREMENT INSTRUMENT IDENTIFICATION NUMBER DAAL03-86-K-0082
8c. ADDRESS (City, State, and ZIP Code) P. O. Box 12211 Research Triangle Park, NC 27709-2211	10. SOURCE OF FUNDING NUMBERS PROGRAM ELEMENT NO. / PROJECT NO. / TASK NO. / WORK UNIT ACCESSION NO.

11. TITLE (Include Security Classification)
Quantitative Use of Exciplex-Based Vapor/Liquid Visualization Systems (A Users Manual)

12. PERSONAL AUTHOR(S)
L. A. Melton

13a. TYPE OF REPORT	13b. TIME COVERED	14. DATE OF REPORT (Year, Month, Day)	15. PAGE COUNT
Final	FROM 7/1/86 TO 10/31/87	88/1/14	75

16. SUPPLEMENTARY NOTATION The view, opinions and/or findings contained in this report are those of the author(s) and should not be construed as an official Department of the Army position, policy, or decision, unless so designated by other documentation.

17. COSATI CODES		
FIELD	GROUP	SUB-GROUP

18. SUBJECT TERMS (Continue on reverse if necessary and identify by block number)
Fuel sprays, visualization, fluorescence, exciplex

19. ABSTRACT (Continue on reverse if necessary and identify by block number)

This report is written in the form of a users manual for exciplex-based vapor/liquid visualization systems. It attempts to bring together in one handbook all the photophysical functions and parameters specific to the exciplex system which will be needed by a user who is otherwise skilled with planar laser induced fluorescence. In addition, it attempts to identify the major assumptions required for the derivations, to define the experimental conditions under which near quantitative interpretation of the fluorescence is possible, and to recommend protocols for visualization experiments.

The best visualization systems developed so far are based on the exciplex formed between N,N,N',N'-tetramethy-p-phenylenediamine (TMPD) and Napthalene or 1-Methylnapthtalene. For these systems, when used with n-tetradecane as the solvent (fuel), it should be possible to measure the liquid and vapor mass concentrations in a volume element of ± 25%, provided that oxygen is excluded. The functions and parameters given in this manual are those appropriate for these two systems.

20. DISTRIBUTION/AVAILABILITY OF ABSTRACT	21. ABSTRACT SECURITY CLASSIFICATION
☐ UNCLASSIFIED/UNLIMITED ☐ SAME AS RPT. ☐ DTIC USERS	Unclassified
22a. NAME OF RESPONSIBLE INDIVIDUAL	22b. TELEPHONE (Include Area Code) / 22c. OFFICE SYMBOL

DD FORM 1473, 84 MAR 83 APR edition may be used until exhausted. All other editions are obsolete.

SECURITY CLASSIFICATION OF THIS PAGE
UNCLASSIFIED

QUANTITATIVE USE OF EXCIPLEX-BASED VAPOR/LIQUID VISUALIZATION SYSTEMS (A USERS MANUAL)

FINAL REPORT

LYNN A. MELTON

JANUARY 1, 1988

U. S. ARMY RESEARCH OFFICE

CONTRACT DAAL03-86-K-0082

UNIVERSITY OF TEXAS AT DALLAS
P.O. BOX 830688
RICHARDSON, TEXAS 75083

APPROVED FOR PUBLIC RELEASE;
DISTRIBUTION UNLIMITED

ABSTRACT

This report is written in the form of a users manual for exciplex-based vapor/liquid visualization systems. It attempts to bring together in one handbook all the photophysical functions and parameters specific to the exciplex system which will be needed by a user who is otherwise skilled with planar laser induced fluorescence. In addition, it attempts to identify the major assumptions required for the derivations, to define the experimental conditions under which near quantitative interpretation of the fluorescence is possible, and to recommend protocols for visualization experiments.

The best visualization systems developed so far are based on the exciplex formed between N,N,N',N'-tetramethy-p-phenylenediamine (TMPD) and Naphthalene or 1-Methylnaphthalene. For these systems, when used with n-tetradecane as the solvent (fuel), it should be possible to measure the liquid and vapor mass concentrations in a volume element of a fuel spray with absolute accuracies of approximately $\pm$ 25%, provided that oxygen is excluded. The functions and parameters given in this manual are those appropriate for these two systems.

TABLE OF CONTENTS

I. Introduction

A. Purpose of this Manual

Exciplex-based vapor/liquid visualization systems have previously been shown to provide striking qualitative pictures of the separate vapor and liquid patterns around single droplets and in full fuel sprays.[1-5] Those pictures -- or their electronic image analogs -- thus far have provided only qualitative information because there was no quantitative way to relate the measured fluorescence intensities to the vapor and liquid mass concentrations within the volume interrogated. This manual attempts to draw together all the visualization system functions and parameters needed for quantitative interpretation of these fluorescence intensities. It attempts to provide the user -- who can measure experiment-specific quantities such as the incident laser intensity, fluorescence intensities, and spectral response of the filters and detector -- the information necessary to interpret those fluorescence intensities quantitatively in terms of vapor and liquid mass concentrations.

No manual is perfect, and certainly not one which has required the assimilation of as much material as this one. Users are encouraged to communicate suggestions, corrections, additions, and requests for additional information to the author.

B. Overview of Exciplex-Based Vapor/Liquid Visualization Systems

This section is intended to provide a brief overview of the photophysics underlying the exciplex-based vapor/liquid visualization systems. More comprehensive treatments may be obtained from earlier visualization papers or from the original photophysics literature.[6-8]

All exciplex-based vapor/liquid visualization systems are based on the following reversible reaction

$$M^* + G \langle == \rangle E^* \qquad (1)$$

where M^* is the first excited singlet state of a fluorescent organic molecule, the monomer M, which is generally but not always an aromatic molecule, G is an appropriately chosen ground state reaction partner, and E^* is the exciplex. An exciplex -- shortened from excited state complex -- is significantly bound in the excited state, with binding energies of 4-20 kcal/mole, but has no significant binding energy between the ground state molecules M and G. Thus, since E^* is bound with respect to separated M^* and G and emits to the same ground state, its emission is necessarily redshifted with respect to the M^* emission, and this shift

may be as much as 100-200 nm. This concept is illustrated in Figure 1.

By setting the concentration of G in the liquid phase sufficiently high, it is possible to drive the equilibrium in equation (1) far to the right, i.e., the emission of E^* from the liquid may be a hundred times that of M^*. In the vapor, the relatively polar exciplex -- an excited state charge transfer complex -- is much less stable, and the concentrations are much lower; as a result, in the vapor the emission from M^* may be a hundred times that of E^*. These two facts taken together, distinct emissions from M^* and E^* and the identification of M^* emission with the vapor phase and E^* emission with the liquid phase, mean that a filter which isolates the M^* emission enables one to photograph the vapor pattern, and a filter which isolates the E^* emission enables one to photograph the liquid pattern. Thus the control of the monomer/exciplex equilibrium allows the separate two-dimensional, real-time, non-perturbative visualization of the vapor/liquid concentrations in a fuel spray.

The exciplex-forming dopants, M and G, are dissolved in a solvent which is called F, the fuel. With a properly developed exciplex-based vapor/liquid visualization system, M, G, and F evaporate in a fixed and known relationship, and thus the total vapor concentration (M, G, and F) may be calculated from the fluorescence of M^*. The liquid phase fluorescence from E^* is taken to be directly proportional to the total liquid concentration.

The above discussion has emphasized vapor and liquid concentrations rather than the droplet size distributions and number densities usually associated with studies of fuel spray evaporation. The exciplex-based techniques are not sensitive to the droplet size *per se*; all the liquid mass in a given volume will contribute linearly to the fluorescence signal, regardless of whether it is one large droplet or is dispersed into a thousand small droplets. As an aside, the same exciplex chemistry can be used to produce optical thermometers.[9-11] These properties, 1) sensitivity to vapor and liquid masses but not to droplet sizes and number densities, and 2) sensitivity to droplet temperature, show that the exciplex-based visualization techniques are complementary to droplet sizing techniques based on Mie scattering. In all likelihood, both techniques will be needed for the full understanding of the evaporation of fuel sprays.

As a matter of notation, the initial liquid phase composition of an exciplex-based vapor/liquid visualization system will be specified as x M/y G/z F, where x, y, and z are the percentages by weight of M, G, and F in the solution, respectively.

II. Recommended Vapor/Liquid Visualization Systems

Two exciplex-based vapor/liquid visualization systems are recommended in this manual; they are based upon the exciplex formed between N,N,N',N'-tetramethyl-p-phenylenediamine (TMPD) and naphthalene (N) or between TMPD and 1-methylnaphthalene (1MN). The first system, 1 TMPD/10 N/89 T -- the notation means 1% TMPD, 10% N, 89% tetradecane (T) by weight-- is the exciplex with which we have the most experience. The second system, 1 TMPD/10 1MN/89 T, which uses 1MN to provide a better match of boiling points, is expected to be very similar photophysically to the first. Although much of the characterization of the first exciplex system has been done with hexadecane as the solvent, the substitution of tetradecane is not expected to alter the photophysical properties significantly.

The development of an exciplex-based vapor liquid visualization system involves selection of molecules which will form a strongly bound, strongly emitting exciplex, with few other photophysical/photochemical pathways available for decay. More volatile systems require smaller component molecules, while more strongly bound systems generally require larger component molecules. Once the exciplex system is chosen, it must be matched with an appropriate alkane fuel, so that the evaporation of the fluorescent vapor phase marker, M, will track the evaporation of the fuel F, the major component. The result of these multiple constraints is a system which allows very few additional modifications; users should avoid alterations which could jeopardize the compromises which have been made. On the other hand, in many cases, users will either have knowledge of one of the system variables from some other source, or will not require the full vapor/liquid visualization; in these situations, the problem can be much more feasible, and users are encouraged to contact the author regarding alternate, less constrained visualization systems.

Other exciplex-based vapor/liquid visualization systems are under development, particularly ones which may be used to follow the evaporation of fuels with boiling points in the range 0-150 C.

III. Relation of Measured Fluorescence to Vapor and Liquid Concentrations

A. Basic Equations

Assume that the sheet of laser light is propagating in the -X direction in the X-Y plane and that the fluorescence is viewed along the Z axis, as shown in figure 3. Then the fluorescence signal $S_f(x,y,z,L,DL)$ in photons/sec,

originating at some volume element (voxel) in the fuel spray, centered at the point (x,y,z) with edge lengths Dx, Dy, and Dz, respectively, into bandwidth DL about the wavelength L is as follows:

$$S_{+}(x,y,z,L,DL) = I(x,y,z,L_{o*}) * Dy * Dz *$$

$$[< F'_{abs-l}(T,C_l,L_{o*}) * H_l(n,\varepsilon',f\#)> *$$

$$< A(L) * Q'_{+-l}(T,C_l,L),\ DL >$$

$$+ F'_{abs-v}(T,C_v,L_{o*}) * H_v(f\#) *$$

$$< A(L) * Q'_{+-v}(T,C_v,L),\ DL >]$$

(2)

where

$I(x,y,z,L_{o*})$ = number of photons/cm²-sec incident on the voxel at wavelengths between L_{o*} and $L_{o*}+dL$;

$F'_{abs-l}(T,C_l,L_{o*})$ = fraction of the light incident on the voxel at L_{o*} which is absorbed within the voxel by the liquid at temperature T and composition C_l;
$F'_{abs-v}(T,C_v,L_{o*})$ is defined analogously;

$H_l(n,E',f\#)$ = fraction of the photons emitted in a liquid droplet with index of refraction n and absorptivity ε' (cm²/gram) which enter a lens aperture of f-number f#. ε' is a function of L_{o*} and C_l. F'_{abs-l} and H_l actually require convolution, denoted by the angle brackets, which is discussed in section II.C.2.a. $H_v(f\#)$ is the fraction of emitted photons from the vapor within the voxel which enter a lens aperture of f-number f#;

A(L) = fraction of photons at wavelength L, emitted into the lens aperture, which are detected; includes spectral response of lenses, filters, photocathodes, etc.;

$Q'_{+-l}(T,C_l,L)$ = fraction of excited states in the liquid at temperature T and composition C_l which emit at wavelength L per unit wavelength. The quantity $< A(L) * Q'_{+-l}(T,Cv,L),\ DL >$ denotes an integral between L-DL/2 and L+DL/2 with respect to L. $Q'_{+-v}(T,C_v,L)$ and its corresponding integral are defined analogously;

C_l and C_v are vectors of weight fractions of the major species which may be present: M, G, F, N_2, O_2, and in combusting sprays, H_2O and CO_2.

Ideally, F'_{abs-l} and F'_{abs-v} will be linearly proportional to the masses of liquid and vapor in the voxel, respectively, and and thus equation (2) will be the basis

for the quantitative two-dimensional visualization of the separate liquid and vapor fractions of an evolving fuel spray.

B. Assumptions

Equation (2) implicitly includes the following three assumptions:

A1) The radial gradients of temperature and composition within droplets can be neglected.

A2) The droplet temperature and composition do not depend on the droplet size.

A3) Resonances such as those observed by Owen et al.[12] are negligible in both the absorption and fluorescence processes.

These three conditions are necessary to insure that the measured liquid phase fluorescence is directly proportional to the total liquid mass in the voxel. They are both appropriate and reasonable. Internal gradients would be averaged out in the visualization of a system as complex as an evolving fuel spray. Small droplets and large droplets are assumed to have the same temperature, which likely will be true except in the earliest stages of the fuel spray. The boiling points of M, G, and F have been carefully matched in the exciplex-based visualization systems recommended here, and thus small droplets, which may have resulted from the evaporation of large droplets, are assumed not to be different, except for size, from their predecessors. The resonances observed by Owen et al. in the fluorescence of droplets required great uniformity in droplet generation and are quite likely to average out their effects if a significant number of droplets are present in the voxel.

Equation (2) includes functions such as $F_{\bullet\bullet\bullet,-1}$, $F_{\bullet\bullet\bullet,-v}$, H_1, $Q'_{\bullet,-1}$, and $Q'_{\bullet,-v}$, which may depend upon the temperature and/or the vapor/liquid composition. Unless these quantities are independent of temperature and the droplet compositions are independent of time, the vapor and liquid mass concentrations will be confounded with these other variables in the evolving fuel spray, and it will be difficult to obtain information about the mass concentrations alone. Two other assumptions are thus necessary:

A4) The temperature dependence of d_l (the liquid phase density), $F_{\bullet\bullet\bullet,-1}$, $F_{\bullet\bullet\bullet,-v}$, H_1, $Q'_{\bullet,-1}$, and $Q'_{\bullet,-v}$ can be neglected.

A5) C_1 is independent of time, and the material evaporating from the droplets -- M, G, and F -- does so at the composition of the droplet. C_v will change with time as

material evaporates from the droplet and mixes with the ambient atmosphere.

The fourth assumption states that the absorbance and fluorescence strengths of the vapor and liquid phase dopants do not depend on the temperature; this is not rigorously true, and can be particularly significant for $Q'_{f,-1}$. The dependence of these quantities on temperature and the estimated effect on the quantitative interpretation of the fluorescence signals will be discussed in section IV. The fifth assumption, which is coupled with the first two, indicates that the history of a particular droplet or parcel of vapor is irrelevant; the fuel liquid or vapor is measured by the present mass of its marker only.

These five assumptions may be significantly relaxed if single isolated droplets are studied. However, they are necessary and reasonable for a system as complex as an evolving fuel spray.

In most visualization studies a sixth condition is appropriate:

A6) The spray is optically thin, i.e., weakly absorbing and weakly scattering, so that the incident laser intensity is essentially constant across the spray.

By choice of either dopant concentrations or the laser wavelength, one can often achieve optically thin conditions, and with such conditions, it is much easier to insure that the fluorescence from a voxel is directly proportional to the vapor or liquid mass.

C. Detailed Equations

1. Laser Intensity

Under the assumption that the system is optically thin, $I(x,y,z,L_{ex})$ is independent of x. If the laser sheet is uniform in y and centered at z_0, then the laser intensity becomes $I(z_0,L_{ex})$.

2. Absorption and Emission into Lens Aperture

a. Liquid

Under optically thin conditions the number of photons which are absorbed by a liquid droplet of radius r_l and index of refraction n, and which are re-emitted into the aperture of a circular lens of f-number f# is

$$N_l = I(z_0,L_{ex}) * \pi * r_l^2 * \langle F''_{ex,-1}(T,C_l,L_{ex},x_d,y_d,z_d) * H''_l(n,\varepsilon',f\#,x_d,y_d,z_d)\rangle * Q'_{f,-1}(T,C_l,L,DL) \quad (3)$$

The entering rays are refracted and therefore the interior of the droplet is not uniformly illuminated. Similarly, the probability that a photon will escape from the droplet and be refracted into the aperture of the collecting lens is not uniform within the droplet. The functions $F''_{s,s,-1}$ and H''_1 are therefore explicit functions of the coordinates within the droplet -- x_s, y_s, z_s -- and N_1 depends on a triple integral over these coordinates, which is denoted by the angle brackets. Ray tracing calculations, which are summarized in section IV.A.1, show that under optically thin conditions and for fixed n and f#,

$$\langle F''_{s,s,-1} * H''_1 \rangle = k(T,C_1,n,f\#) * \varepsilon' * (2 * r_1) \qquad (4)$$

Thus,

$$N_1 = I(z_0,L_{s,s}) * \pi * r_1^2 * k(T,C_1,n,f\#) * \varepsilon' * (2 * r_1) * Q'_{s,-1}(T,C1,L,DL) \qquad (5)$$

or

$$N_1 = I(z_0,L_{s,s}) * [(3 * k(T,C_1,n,f\#) * \varepsilon')/(2 * d_1(T,C_1))] * Q'_{s,-1}(T,C_1,L,DL) * M_{s,1} \qquad (6)$$

where $M_{s,1}$, the mass of droplet i, $= 4/3 * \pi * d_1(T,C_1) * r_1^3$, and the quantity in square brackets -- which we define as the function $\langle F*H \rangle_1(T,C_1,n,\varepsilon',f\#)$ -- does not depend upon the droplet radius. $d_1(T,C_1)$ is the density of the liquid in the droplet. If the droplets are small compared to the voxel dimensions, so that the probability of a droplet intersecting the voxel surface(s) is small, then a sum over the droplets gives the the total number of photons absorbed and re-emitted into the lens aperture as

$$N_{1,t} = I(z_0,L_{s,s}) * \langle F*H \rangle_1(T,C_1,n,\varepsilon',f\#) * Q'_{s,-1}(T,C_1,L,DL) * M_1(x,y,z_0) \qquad (7)$$

where $M_1(x,y,z_0)$ is the total liquid mass in the voxel. The average liquid mass concentration, $m_1(x,y,z_0)$, may be defined as $M_1(x,y,z_0)/(Dx * Dy * Dz)$.

b. Vapor

Under optically thin conditions, the number of photons absorbed by the vapor in the voxel is

$$N_v = I(z_0,L_{s,s}) * Dy * Dz * \{[(2.303 * \varepsilon') * (C'_v(M)] * m_v(x,y,z_0)) * (Dx)\} \qquad (8)$$

where the terms in parentheses correspond to the quantities required for Beer's Law. $C'_v(M)$ is the weight fraction of M in the vapor computed on the basis of M, G, and F only. $m_v(x,y,z_o)$ is the mass concentration of the vapor. The quantity in square brackets is the specific fraction absorbed by the vapor, $F_{\ldots-v}(T,C_v,L_{ex})$.

$$N_v = I(z_o,L_{ex}) * F_{\ldots-v}(T,C_v,L_{ex}) * M_v(x,y,z_o) \qquad (9)$$

where $M_v(x,y,z_o)$ is the total mass of vapor (M, G, and F) in the voxel.

For the isotropic emission from the homogeneous vapor in a voxel, whose dimensions are small compared to those of the collecting lens, the fraction of the emission falling within the aperture of a circular lens with f-number f# is

$$H_v(f\#) = (4 * f\#)^{-2} \qquad (10)$$

3. Wavelength Selectivity

The quantities $Q'_{f-l}(T,C_l,L)$ and $Q'_{f-v}(T,C_v,L)$ may be decomposed into the product of an overall emission quantum yield and a spectral yield as follows:

$$Q'_{f-l}(T,C_l,L) = Q_{f-l}(T,C_l) * G_l(T,C_l,L) \qquad (11a)$$

$$Q'_{f-v}(T,C_l,L) = Q_{f-v}(T,C_v) * G_v(T,C_v,L) \qquad (11b)$$

where $G_l(T,C_l,L)$ and $G_v(T,C_v,L)$ are normalized such that their integrals over all wavelengths are unity. For small Dl, $G_l(T,C_l,L) * DL$ and $G_v(T,C_v,L) * DL$ are the fractions of photons emitted into a bandwidth DL about the wavelength L by the liquid and vapor, respectively. The spectral yield functions $G_l(T,C_l,L)$ and $G_v(T,C_v,L)$ provide the striking selectivity of the vapor/liquid visualization systems. Q_{f-l} and Q_{f-v} are the absolute quantum yields for fluorescence from the liquid and vapor, respectively.

4. Complete Equations

The results in equations (7), (9), (10), and (11) can now be substituted into equation (2) to give the following full equations for the signal observed at two different wavelengths, L_E and L_M, corresponding to the observation of exciplex and monomer emissions, respectively.

$$S_f(x,y,z_o,\ L_E,DL) = I(z_o,L_{ex}) *$$

$$\{\ [\langle F*H\rangle_l(T_o,C_{lo},n,\varepsilon',f\#) * Q_{f-l}(T_o,C_{lo}) *$$

$$\langle A_E(L) * G_l(T_o,C_{lo},L),\ DL\rangle] * M_l(x,y,z_o) +$$

$$[F_{abs-v}(T_o, C_{v,o}, L_{ex}) * H_v(f\#) * Q_{f-v}(T_o, C_v) *$$

$$\langle A_E(L) * G_v(T_o, C_{v,o}, L),\ DL\rangle] * M_v(x, y, z_o) \} \quad (12a)$$

$$S_f(x, y, z_o, L_M, DL) = I(z_o, L_{ex}) *$$

$$\{ [\langle F*H\rangle_l(T_o, C_{l,o}, n, \varepsilon', f\#) * Q_{f-l}(T_o, C_{l,o}) *$$

$$\langle A_M(L) * G_l(T_o, C_{l,o}, L),\ DL\rangle] * M_l(x, y, z_o) +$$

$$[F_{abs-v}(T_o, C_{v,o}, L_{ex}) * H_v(f\#) * Q_{f-v}(T_o, C_v) *$$

$$\langle A_M(L) * G_v(T_o, C_{v,o}, L),\ DL\rangle] * M_v(x, y, z_o) \} \quad (12b)$$

The designations T_o, $C_{l,o}$, and $C_{v,o}$ indicate that a single value, rather than a time-dependent value, can be used for these parameters. Note that Q_{f-v} has an explicit dependence upon the time-dependent C_v, since molecular oxygen is very effective in quenching the emitting M* state.

$A_E(L)$ and $A_M(L)$ now include filters which isolate the wavelengths L_E and L_M, respectively.

D. Application Equations

Equations (12a) and (12b) can be written more compactly as follows:

$$S_f(x, y, z_o, L_E, DL)/I(z_o, L_{ex}) =$$

$$B_l(L_E) * M_l(x, y, z_o) + B_v(L_E) * M_v(x, y, z_o) \quad (13a)$$

$$S_f(x, y, z_o, L_M, DL)/I(z_o, L_{ex}) =$$

$$B_l(L_M) * M_l(x, y, z_o) + B_v(L_M) * M_v(x, y, z_o) \quad (13b)$$

where $B_l(L_E)$, $B_v(L_E)$, $B_l(L_M)$, and $B_v(L_M)$ correspond to the terms collected in square brackets in equations (12a) and (12b). $M_l(x, y, z_o)$ and $M_v(x, y, z_o)$ are the total liquid mass and the total vapor mass in the voxel centered at (x, y, z_o), respectively.

The proposed visualization systems have been designed so that there exist wavelengths L_E and L_M such that emission at L_E is almost entirely from the liquid and emission at L_M is almost entirely from the vapor. Mathematically, this means that

$$G_l(T, C_l, L_E) >> G_v(T, C_v, L_E) \quad (14a)$$

$$G_l(T, C_l, L_M) << G_v(T, C_v, L_M) \quad (14b)$$

Thus, at L_g the first term in the sum in equation (13a) dominates the measured fluorescence signal, and at L_m the second term in equation (13b) dominates the signal. In the event that the minor terms are truly negligible, the following approximate equations result:

$$S_f(x,y,z_o,L_g,DL)/I(z_o,L_{ex})] = B_l(L_g) * M_l(x,y,z_o) \quad (15a)$$

$$S_f(x,y,z_o,L_m,DL)/I(z_o,L_{ex})] = B_v(L_m) * M_v(x,y,z_o) \quad (15b)$$

Equations (15a) and (15b), when applicable, allow the direct photographic visualization of the separate liquid and vapor patterns in an evolving fuel spray. When the full equations (13a) and (13b) must be used, i.e., when the minor terms are not negligible, $M_l(x,y,z_o)$ and $M_v(x,y,z_o)$ are obtained as solutions of the two linear equations, (13a) and (13b), at each point (x,y,z_o).

The arrangement of equations (13a) and (13b) partially delineates the responsibilities of the users and of the developers of the exciplex-based visualization systems. The functions on the left hand side -- $S_f(x,y,z_o,L,DL)$ and $I(z_o,L_{ex})$ --- are properties of the experiment rather than the visualization system, and hence will be determined by the user in the course of a spray diagnostic experiment. The functions on the right hand side, the B coefficients -- or more particularly their detailed components F, H, Q, and G -- are properties of the exciplex-based visualization system, and will be determined as part of the photophysical characterization of that system. A user will still have to calculate the integrals of the G functions over the spectral response functions A(L) for the particular detection system. The estimation/ calculation of these functions/parameters for the specific exciplex-based vapor/liquid visualization systems recommended here is treated in section IV of this report.

IV. Calculation/Estimation of B coefficients

A. Functions

1. $\langle F*H\rangle_l(T,C_l,n,\varepsilon',f\#)$

As noted in the derivations of equations (3)-(7),

$$\langle F*H\rangle_l(T,C_l,n,\varepsilon',f\#) = (3 * k(T,C_l,n,f\#) * \varepsilon')/(2 * d_l(T,C_l)) \quad (16)$$

where $k(T,C_i,n,f\#)$ is derived from a triple integral over the internal coordinates of a droplet having index of refraction n, and mass absorptivity ε', and which emits into a lens aperture f#. $d_i(T,Cl)$ is the density of the solution. For this work, it may be evaluated at room temperature and assumed to be temperature independent.

The derivation of the value of $k(T,C_i,n,f\#)$ is quite complex and will be the subject of a separate paper. A brief description of the physics should suffice here. A droplet acts as a converging lens, and hence a droplet which is subjected to a uniform intensity of collimated light focuses these rays toward the non-illuminated side of the droplet. These effects have been shown quite dramatically by Benincasa et al.[13] A corollary of this effect is that the probability of a photon, which is emitted isotropically, being refracted into the aperture of a collecting lens also depends upon location of the emitter within the droplet. The total number of photons emitted into the lens aperture is then computed by determining the number of photons absorbed in each grid element of a droplet, and the probability of detection of the isotropically emitted photons from each grid element, and by summing the product of these two quantities over all grid elements. The probability of detection of a photon does not depend upon the droplet optical density -- D.O.D. = $E' * m(M) * (2 * r_i)$, where r_i is the radius of the droplet. For optically thin droplets, the distribution of absorption within the droplet does not depend upon the optical density, but the total absorption -- and total emission -- are proportional to D.O.D.

Figure 4a shows a log-log plot of the fraction of the incident light which is refracted into a droplet with index of refraction n = 1.40, absorbed, and emitted into a lens aperture f# = 3.5 -- the quantum yield is taken as unity -- versus the droplet optical density. The linear behavior observed for D.O.D. < 0.1 shows that the fraction is proportional to D.O.D., i.e., equations (4) - (7). At D.O.D. of approximately 3, the fraction reaches a maximum and then declines; the incident light is absorbed close to the front surface and out of the region of maximum detectability. Figure 4b shows a portion of the same data plotted in a linear format. In terms of the slope, $k'(T,C_i,n,f\#)$, of the linear portion of figure 4b,

$$k(T,Cl,n,f\#) = k'(T,C_i,n,f\#) * C_i(M) * d_i(T,C_i) \qquad (17)$$

or

$$\langle F*H\rangle_i(T,C_i,n,\ ',f\#) =$$

$$[1.5 * k'(T,C_i,n,f\#) * C_i(M) *\ '] \qquad (18)$$

Because the calculation is complex and the procedure is not generally available, we have listed in Table I the values of $k'(T,C_l,n,f\#)$ for a selection of values of the index of refraction and f# which may be encountered. The variation with N is quite small; the dominant variation is with f#. The values in Table I can be fit by equation (19) within $\pm$ 15%.

$$k'(T,Cl,n,f\#) = [0.115 - 0.8*(n - 1.40)] * f\#^{-2.40} \quad (19)$$

It should be noted that $k'(T,C_l,n,f\#)$ actually depends upon n and f# only. The dependence of $\langle F*H\rangle_l$ on T and C_l arises from the dependence of n and E' on these quantities. The values given in Table I are for an experiment in which the detector is located at 90° with respect to the illuminating laser beam; different values would be obtained for other experimental geometries.

2. $F_{abs-v}(T,C_v,L_{ex})$

If the system is optically thin, then the approximate expression defined in equations (8) and (9) is appropriate. In general the number of photons absorbed in the voxel is

$$N_v(x,y,z_0) = I(x,y,z_0,L_{ex}) * DyDz * [\,1 - 10^{(-V.O.D.)}\,] \quad (20)$$

where $V.O.D. = \varepsilon'(L_{ex}) * (C'v(M) * m(x,y,z0)) * Dx)]$

V.O.D. is the vapor optical density. ε' is the mass concentration analog of the molar extinction coefficient and has the units of volume/gram-cm, i.e., $cm^2/$(gram of absorber). Section IV.B.3 provides more information on '. $C'_v(M) * m(x,y,z_0)$ is the mass concentration of the assumed sole absorber, M, in grams/cm^3; $C'_v(M)$ is the mass fraction of M in the vapor, computed on the basis of M, G, and F only, and $m(x,y,z_0)$ is the total mass concentration of M, G, and F in the voxel. Dx is the length of the voxel in cm. Mass concentration units were chosen here, instead of the more common molar concentration units, because when these systems are used with real fuels, it is often not possible to define the molar composition of the solution.

3. $H_v(f\#)$

Under the assumptions that the voxel is small compared to the dimensions of the collecting lens and that the index of refraction of the vapor portions of the evaporating fuel spray is unity, geometrical arguments are

sufficient to calculate the fractional solid angle subtended by the lens aperture:

$$H_v(f\#) = (4 * f\#)^{-2} \qquad (21)$$

This formula is written in terms of the effective lens aperture. If the voxel is at the focal point of the lens, f# is the f-number of the lens; for other cases, f# is the ratio of the distance from the voxel to the limiting optical aperture to the diameter of that aperture.

4. $G_l(T,C_l,L)$

$G_l(T,C_l,L)$ may be derived from the spectrally corrected fluorescence spectrum $F_{corr-l}(L)$ for a liquid sample at temperature T and composition C_l by use of the following formula:

$$G_l(T,C_l,L) = F_{corr-l}(L) \Big/ \int_0^{\infty} F_{corr-l}(x)dx \qquad (22)$$

The spectrally corrected fluorescence spectra for the systems recommended in this report are given for a series of temperatures in Figures 5a-5i, where, for ease of display, each figure is normalized to a common maximum. The spectra for the 1 TMPD/ 10 N/89 T and 1 TMPD/ 10 1MN/89 T systems are expected to be similar. For computations, $G_l(T,C_l,L)$ is listed following each figure.

A survey of the spectra in Figures 5a-5i shows that the liquid phase fluorescence spectra are somewhat temperature dependent. Two effects are present: the exciplex emission shifts slightly to higher energies as the temperature increases, and the emission from the monomer begins to emerge, since the monomer/exciplex equilibrium constant decreases as the temperature increases. As noted in the derivation of equation (12), it is necessary to choose some temperature T_0 at which to evaluate these functions. At present T_0 approximately equal 150 C is recommended since it provides a reasonable balance between the shift of the exciplex emission and the decrease of $Q_{e-l}(T,C_l)$.

5. $G_v(T,C_v,L)$

$G_v(T,C_v,L)$ may be derived from the spectrally corrected fluorescence spectrum $F_{corr-v}(L)$ for a vapor sample at temperature T and composition C_v by use of the following formula:

$$G_v(T,C_v,L) = F_{corr-v}(L) \Big/ \int_0^{\infty} F_{corr-v}(x)dx \qquad (23)$$

The spectrally corrected fluorescence spectrum for TMPD is given in Figure 6, where, for ease of display, the figure is normalized. For computations, $G_v(T,C_v,L)$ is listed following the figure.

Unlike the liquid, the normalized vapor phase spectrum is virtually independent of temperature and composition, and thus a single spectrum is provided.

6. C_l and C_v

C_l and C_v are vectors of weight fractions of M, G, F and, in the vapor, N_2, O_2, and possibly CO_2 and H_2O. The weight fraction of a component J is defined as follows:

$$C(J) = m(J)/[m(M) + m(G) + m(F) + m(N_2) + m(O_2) + \ldots] \quad (24)$$

where m(J) is the mass concentration of component J in the voxel.

$C'_v(M)$ is the mass fraction of M in the vapor computed on the basis of M, G, and F only.

B. Parameters

1. $Q_{l-l}(T,C_l)$

The absolute quantum yield for fluorescence as a function of temperature has been determined for the 1 TMPD /10 N/89 H exciplex system by means of a two part experiment.[14] The absolute quantum yield at room temperature was determined by comparison of the corrected fluorescence with the corrected fluorescence of standards of known quantum yield. The relative quantum yields of the exciplex as a function of temperature were then determined and were normalized to the known absolute value at room temperature. This work will be the subject of a separate paper. The exciplex has no bound ground state, and hence cannot absorb photons directly; the quantum yields reported here are the number of photons emitted by the exciplex per photon absorbed by M and/or G. The same room temperature quantum yield was obtained with either hexadecane or cyclohexane, and the substitution of tetradecane as a solvent is expected to have negligible effect also.

Figure 7 shows the absolute quantum yield for fluorescence for the 1 TMPD/ 10 N/89 H system as a function of temperature. Ideally the quantum yield would be independent of temperature; in fact, it is virtually independent of temperature up to approximately 150 C and then falls by about 30% as the temperature increases to 250 C.[14] It is recommended that the value 0.15 be used as a

reasonably weighted average value for the 1 TMPD/10 N/ 89 T system.

A value of 0.05 ± 0.002 is recommended for the absolute quantum yield of the 1 TMPD/10 1MN/89 T system.[14] This system is expected to have a temperature dependence of its quantum yield which is similar to that shown in Figure 7.

It should be noted that the quantum yields were measured in solutions which had been carefully purged with N_2 to remove the atmospheric O_2, which will strongly quench the exciplex fluorescence. Air-saturated solutions show approximately 10% of the fluorescence obtained from N_2 purged solutions.

2. $Q_{f-v}(T,C_v)$

For a properly chosen value of L_{ex}, only the TMPD will be excited in the vapor (see also section IV.B.5). However, the value of $Q_{f-v}(T,Cv)$ may vary dramatically with composition, primarily because of quenching of the TMPD fluorescence by O_2.

The fluorescence S_f from a molecule M is affected by composition as shown in the following equation:

$$S_f = b' * [A * \tau] * I_o * P_M * [\,1 + \tau * (\,\sigma\ K_q(i) * P_i\,)\,]^{-1} \qquad (25)$$

where

b′ is a constant which includes absorptivities, collection efficiencies, etc.

A = radiative rate constant; K_i = sum of the rate constants for internal conversion and intersystem crossing, and τ (the radiative lifetime) = $(A + K_i)^{-1}$. Note that it is not necessary to know in order to determine Q_{f-v}.

P_i = pressure of component i in torr.

$K_q(i)$ = rate constant for quenching of M* by i, with units $torr^{-1}\ sec^{-1}$.

The sum is over all components present: M, G, F, O_2, N_2, and possibly CO_2 and H_2O. In this work, M = TMPD, and G = N or 1MN.

The best current values for the rates times tau, in units of $torr^{-1}$, are as follows: $K_q(M) * \tau < 0.01$ (measured)[13]; $K_q(G) * \tau = 0$ (see discussion below); $K_q(F) * \tau = 0$ (estimated, see discussion below); $K_q(O_2) * \tau = 0.103 \pm 0.006$ (measured)[14]; $K_q(N_2) * \tau = 0$ (estimated, see

discussion below); $K_q(CO_2) * \tau < 6 \times 10^{-5}$ (measured)[16]; and $K_q(H_2O) * \tau = 0$ (estimated, see discussion below). The measured rates will be discussed in a subsequent paper.

For virtually all fluorescent aromatic molecules, alkanes and nitrogen produce negligible quenching of fluorescence, presumably because they have no accessible electronic states to which M* can transfer energy and because singlet to triplet energy transfer is spin-forbidden. CO_2 and H_2O are expected to follow this pattern also, but much less data is available for these quenchers. Molecular oxygen is, however, an efficient quencher since the triplet oxygen can cause the excited organic molecule to transfer from its singlet excited state to a nearby triplet excited state.[17] Clearly G interacts with M* --the exciplex formation reaction in the liquid-- but the exciplex is sufficiently unstable in the vapor (no exciplex emission is observed in these vapors) that the reverse reaction rate is fast compared to the forward reaction rate; the net effect may be treated here by setting $K_q(G) = 0$. The rates are expected to exhibit only a very weak temperature dependence since the processes are exothermic.

The effect of these quenching processes may be summarized as follows:

$$Q_{f-v}(T,Cl) = Q_{f-v}(TMPD) * [\ 1 + 78.3 * P(O_2)_{atm}\ ]^{-1} \qquad (26)$$

where $Q_{f-v}(TMPD)$ is the quantum yield of TMPD in the absence of any collisional quenching. $Q_{f-v}(TMPD)$ has not been measured, and hence $Q_{f-l}(TMPD) = 0.13 \pm 0.02$, which has been measured in non-polar liquid,[14] is recommended for the present as an estimate of $Q_{f-v}(TMPD)$. $P(O_2)_{atm}$ is the partial pressure of oxygen in atmospheres.

Note that the effect of quenching by molecular oxygen is quite severe. An experiment run into air at one atmosphere, where $P(O_2)_{atm} = 0.21$, will result in a reduction of Q_{f-v} from its unquenched value by a factor of approximately seventeen.

The value of $K_q(M) * \tau$ was obtained from the analysis of experiments in which $P_{TMPD} <= 15$ torr.[15] However, for an experiment at one atmosphere using the 1 TMPD/10 N/89 T visualization system, the expected pressure of TMPD in the vapor is less than 8 torr. Thus self quenching is expected to be negligible, and, provided the system is optically thin, the vapor phase fluorescence is expected to be linear in P_{TMPD}, or alternately, in the mass of TMPD within the voxel.

3. ε_1' and ε_v'

The molar absorptivities of N, 1MN, and TMPD as a function of wavelength are shown in figures 8-10. In general, these quantities are very weak functions of temperature and composition, provided all components of the solution are non-polar, and thus the room temperature spectra may be used for virtually any fuel spray applications. The long wavelength edge of the absorption band is in general the most sensitive portion, since additional absorption from thermally excited levels of the ground state may contribute additional absorption ("hot bands").

The molar absorptivities (liters/mole-cm) may be converted to mass concentration absorptivities (cm^2/(gram of absorber)) as follows:

$$\varepsilon'(cm^2/gram) = \varepsilon(liters/mole\text{-}cm) * 1000/MW \qquad (27)$$

where MW is the molecular weight of the absorbing species.

The absorptivity in the vapor is not expected to be greatly different from that in a nonpolar solvent such as an alkane. However, since, in the course of other experiments, the vapor phase absorptivities of TMPD have been measured at the long wavelength edge of the absorption band,[15] they are presented in Table II.

4. Index of Refraction

The index of refraction, n, is needed for the droplet absorption-emission calculations. However, as shown in table I, $f'(T,C_1,n,f\#)$ is not very sensitive to the value of n, and hence an reasonably estimated approximate value is adequate. Table III lists values of the index of refraction for several of the common solvents.[18] If extrapolation to shorter wavelengths is necessary, it is probably appropriate to use the formula reported by Berlman for cyclohexane,

$$(n^2 - 1)^{-1} = a - b * x' \qquad (28)$$

where for cyclohexane, a = 0.9965, b = 0.01025, $x' = \nu^2 * 10^{-8}$, and ν = the frequency in wavenumbers.[19]

5. L_{ex}

The photophysics of these exciplex-based vapor/liquid visualization systems depend upon the excitation wavelength L_{ex} in two ways: ε' is a function of L_{ex} and, at sufficiently short wavelengths, both M and G may be excited (and thus fluoresce) in the vapor.

$\varepsilon'(L)$ in general increases dramatically at wavelengths below 300 nm (see figures 8-10), and thus at longer wavelengths, there is a better chance of maintaining optically thin conditions. Quantitative interpretation of the measured fluorescence intensities is much more difficult if the system is not optically thin. However, too large a value of L_{ex} can result in unacceptably high levels of scattered laser light in the vapor phase fluorescence band. In the 1 TMPD/10 N/89 T visualization system, if L_{ex} < 325 nm, it is possible to excite the naphthalene as well as the TMPD. In this case, at low mass concentrations, the vapor phase spectra may be that of naphthalene (L_{em} = 340 nm); at higher mass concentrations the excited naphthalene transfers its energy to TMPD and the vapor phase spectrum becomes that of TMPD (L_{em} = 390 nm).

6. L_ε and L_M

Three major criteria influence the choice of L_ε and L_M, the wavelengths at which the liquid and vapor emissions are approximately measured, respectively: the desire to reject all vapor emission when measuring the liquid emission (and vice versa), the need to obtain a strong signal, and the need to reject scattered light from the exciting laser. For the 1 TMPD/10 N/89 T vapor/liquid visualization system, reasonable choices may be deduced from figures 5a-5x and 6. TMPD does not emit at wavelengths longer than 500 nm; thus a filter which cuts off all emission below 500 nm and passes that above 500 nm will satisfy the criteria nicely. (YAG users should consider how to get rid of the seemingly ubiquitous 533 nm light which accompanies the tripled and quadrupled beams; a more selective filter may be necessary here). A bandpass filter centered at 390 nm, and strongly blocked on the low wavelength side, will allow most of the TMPD emission (from the vapor) through, and indeed, vapor signal tends to be limiting factor. However, such a filter will also allow a minor fraction of the emission from the liquid to pass, and this will have to be subtracted out of the apparent vapor signal in order to obtain a quantitative vapor mass concentration.

Bardsley et al have reported choices for these filters.[20] A brief summary of their apparatus is given in section V.B.2.

7. $C_v'(M)$

In an exciplex-based vapor/liquid visualization system, the vapor phase mass concentration is determined by measuring the fluorescence of the vapor phase marker, M, which is not the fuel itself. Even if the vapor phase concentration of M is measured accurately, one must still establish that a fixed and known relation exists between the vapor phase concentrations of M and F. The simplest

relation is that $C_v'(M) = C_l(M)$, i.e., the droplet evaporates with M and F in the vapor in the same relation as in the droplet. This section describes methods developed to relate $C_v'(M)$ to C_l.

Calculations of the evaporation of multicomponent droplets show that the rate of heat transfer to the droplet dramatically affects the composition of the vapor coming off the droplet.[21] If the rate of heat transfer is low, so that the rate of regression of the droplet surface is slow compared to the mass transfer mechanisms --diffusion and convection-- within the droplet, the the droplet remains well-stirred, and the vapor is produced as in an equilibrium distillation; the more volatile components come off first. However, if the rate of heat transfer is high, so that the internal mass transfer processes cannot maintain a well-stirred droplet, there is an initial "flash" of the volatiles at the surface, and thereafter the droplet evaporates with each successive layer coming off at approximately the bulk composition of the droplet. The slow evaporation case is therefore the worst case in terms of potential deviations from the ideal relationship $C_v'(M) = C_l(M)$.

The equilibrium distillation of a droplet has been modeled with a modest computer calculation. The solutions have been treated as ideal (obeying Raoult's Law), with component vapor pressures given by the Clausius-Clapeyron equation. The heats of vaporization are in general not known for these compounds, and thus they have been estimated using Trouton's Rule. In the calculations, the initial composition and the boiling points of the components were specified. The boiling temperature at 1 atmosphere pressure was then calculated. 1% of the initial droplet was assumed to evaporate at the vapor pressures appropriate to that temperature. The liquid and vapor compositions were calculated, and the procedure was repeated until the droplet was completely evaporated. These procedures will be described more completely in a subsequent paper.

The results of these distillation calculations were plotted as the percentage of the marker evaporated versus the percentage of the entire droplet evaporated. Figures 11 and 12 show the results for the 1 TMPD/10 N/89 T and 1 TMPD/10 1MN/89 T visualization systems, respectively. The diagonal line represents ideal performance, in which the percentage of the marker evaporated is exactly the same as the percentage of the droplet evaporated. The boiling points are as follows: TMPD, 260 C; N, 218 C; 1MN, 240-243 C; T, 252-254 C. As the figures show, the 1 TMPD/ 10 1MN/ 89 T system, in which the boiling points are more nearly matched, provides more nearly ideal performance. As emphasized in the first paragraph of this section, the equilibrium distillation calculation represents the worst

case in terms of deviation from ideal behavior. If the heat transfer to the droplet is rapid, then the calculated curves in figures 11 and 12 will move toward the diagonal, i.e., toward more nearly ideal evaporation behavior.

8. Radiative Lifetimes

The radiative lifetimes do not enter explicitly into the formulas in section III, and indeed are not necessary to calculate $Q_{i,v}$ in section IV.B.2. However, some knowledge of the lifetimes is necessary to assure that the exciplex-based vapor/liquid visualization system has a response which is fast compared to the motion of droplets and vapor within an evaporating fuel spray. If this is so, then the measurement can be made "instantaneously" and the motion in the spray can be "stopped". If the visualization system is fast, then potentially one can make real-time measurements on evolving fuel sprays.

Berlman lists the decay time of TMPD* in cyclohexane 4.3 nsec.[19] This value is probably correct for solutions in nonpolar fuels and approximately correct for TMPD emission in the vapor phase. Berlman also lists the decay times for excited naphthalene and 1-methylnaphthalene in cyclohexane as 96 and 67 nsec, respectively;[19] at the concentration of TMPD and naphthalenes used in these visualization systems, all these species are quenched to form the exciplex in times on the order of 1 nsec. The exciplex lifetime has been found to be 75 $\pm$ 2 nsec in hexadecane.[22] The longest lifetime in the system, that of the exciplex, is less than 10^{-7} sec. For excitation with a 10-20 nsec laser pulse, typical of YAG and excimer lasers, all the fluorescence will have disappeared in less than 1 microsecond. Thus, the photophysical measurement can be repeated at rates greater than 1 MHz, which are significantly faster than the rates needed for real time measurements in evolving fuel sprays.

V. Experimental Protocols and Apparatus

A. Protocols

1. Exclusion of Oxygen

> Protocol 1: The use of the exciplex-based vapor/liquid visualization systems is recommended only for spray systems in which oxygen is excluded, both in the vapor and in the liquid. The ambient gas should be N_2, and the liquid should be thoroughly purged with N_2 prior to injection.

At the present time, the quenching of the vapor phase fluorescence by molecular oxygen is the factor which limits the use of these exciplex-based vapor/liquid visualization systems in combustion applications. The issue

is not necessarily one of signal strength, because it is often possible to increase the gain on an intensified detector to compensate for the loss of intensity due to quenching. With oxygen quenching, there arises a fundamental ambiguity in the interpretation of the vapor phase intensities: if little fluorescence is seen from a voxel, it may be that there was little vapor there, i.e., not much evaporation took place; or it may be that there were substantial amounts of vapor and oxygen in the voxel, so that a large fluorescence signal was quenched to a small one. In many cases, a user will have knowledge of the fluid dynamics and mixing in the system and may be able to predict that little oxygen is present in a specific zone; in those cases, the visualization systems may be used with confidence even though oxygen is present in the overall system.

2. Optically Thin Systems

Protocol 2: The quantitative interpretation of the intensities measured using the exciplex-based vapor/liquid visualization systems should only be attempted if the spray system is optically thin, i.e., the absorption and scattering are sufficiently weak that the laser beam is not significantly attenuated in crossing the spray.

The arguments developed in sections IV.A.1 and IV.A.2 regarding the proportionality of the fluorescence signals to the mass concentrations apply only to optically thin systems. Substantially more complicated -- and less certain -- formulations would be required to deal with other cases.

3. Sources, Purity, and Handling of Chemicals

Protocol 3: The chemicals described in this manual are commercially available, and may be probably be used as received. They are not strongly toxic but should be treated with caution.

These exciplex systems have been tested with naphthalene , 1-methylnaphthalene, TMPD, tetradecane, and hexadecane purchased from Aldrich Chemical Co., although there is no reason to believe that this is a unique source. The naphthalenes are available in high purity and present no problem. The TMPD is typically available as a sandy-grey solid, of stated 97-98% purity; it may be purified by sublimation to yield a while solid which should then be kept refrigerated and under nitrogen in order to minimize its facile air oxidation. However, the TMPD does not have to be purified in order to use it in these visualization systems; the exciplex spectra do not change with higher purity. (Clearly, at some point purity does matter; the point is that the systems are not very sensitive to impurities.) Once TMPD containing solutions are prepared, they should be

kept purged with N_2 since the air oxidation is faster in solution. Heating accelerates the oxidation, and solutions which have been exposed to air at high temperature will turn yellow and possibly precipitate a brown solid; these should be discarded. The tetradecane and particularly the hexadecane will contain impurities which fluoresce in the absence of N or TMPD. Although these are an important consideration in careful photophysical work, in these visualization systems, the weak impurity fluorescence is usually completely masked by the strong fluorescence from the dopants, TMPD and N (or 1MN), and their exciplex. For careful work, these solvents may be purified by oxidation of the impurities with sulfuric acid, water extraction, and drying.[14,23]

All the chemicals specified here have low toxicity. TMPD is a mild skin irritant, which affects some individuals more than others.[24] The alkane solvents present little chemical hazard, and because they are high boiling, they present little flame hazard. Wash hands after coming in contact with these chemicals, and particularly before eating.

The prior discussion should be taken to indicate that these exciplex-based vapor/liquid visualization are surprisingly robust in response to impurities and are of low toxicity; it is not a license to avoid proper care in the preparation, storage, and use of the solutions.

4. Direct Calibration Methods

Protocol 4: It is recommended that, where possible, users calibrate the sensitivity of their detection system using direct calibration methods instead of the photophysical function/parameter methods described in section IV.

The photophysical function/parameter methods described in section IV are soundly based, but in using them, there is a cumulative error involving physical approximations and errors in the necessary parameters. Direct calibration methods, in which a known liquid or vapor mass can be prepared in a voxel, can give more accurate calibrations. If one is studying single droplets, the direct way to measure the liquid mass is to use microscopy to measure the droplet diameter.[25] This known mass may, if necessary, then be used to determine the proportionality constant, r_1, between the fluorescence signal detected and the product of the droplet mass and the incident laser intensity:

$$S_{f1}(x,y,z,L_E) = r_1 * M_{droplet} * I(x,y,z,L_{ex}) \qquad (29)$$

At present, no spray device is known to the author which would serve as a satisfactory standard for sprays.

Direct calibrations for the vapor are, however, possible. Sealed cuvets can be prepared which contain a known, small amount of TMPD. As the cuvet is heated, the TMPD vaporizes until, at some temperature T_v^* the sample is entirely vaporized. Above T_v^*, the mass concentration of the TMPD is fixed and known, and the cuvet may be used to determine the proportionality constant, r_v, between the fluorescence signal detected and the product of the vapor mass concentration and the incident laser intensity:

$$S_{f,v}(x,y,z,L_m) = r_v * M_v(x,y,z) * I(x,y,z,L_{e,x}) \qquad (30)$$

These procedures will be described in a subsequent paper.

As noted in the opening paragraph of this section, these direct calibration procedures will likely be more accurate than the photophysical calculations.

B. Apparatus

1. General Recommendations

a. Lasers

There is not a unique choice for the excitation laser, and the considerations in this section are intended as a modest guide.

CW/Pulsed Ion Lasers

These lasers offer good beam quality and generally sufficient power. However, photons at the UV lines they produce in the 350 nm range are just barely adequate to excite the TMPD/naphthalene visualization system. Visualization systems which are under development for use with more volatile fuels will probably require excitation at wavelengths near 250 nm, and these lasers, unless they are frequency doubled, would not suffice.

Nd:YAG Lasers

The third and fourth harmonics available from these lasers, at 355 and 266 nm, respectively, provide excellent high power sources with excellent beam quality. Bardsley et al used the 355 nm output from a Nd:YAG laser, instead of the 266 nm output, in order to obtain an optically thin system.[20] The fourth harmonic, however, is not sufficiently energetic to pump the visualization systems which are under development for more volatile fuels. Repetition rate is 10-20 Hz.

Excimer Lasers

The excimer lasers can provide high power, pulsed outputs at 351 nm (XeF), 308 nm (XeCl), 248 nm (KrF), and 193 nm (ArF). The beam quality is poor unless a cavity-injected system is used. The three longer wavelengths are, however, an excellent selection for pumping the current visualization systems and the ones under development for more volatile fuels. Repetition rate is 1-100 Hz, with some models extending to 1 KHz.

Copper Vapor Lasers

These lasers are attractive because of their high pulse rate (1-10 KHz), which is in the range required for real-time monitoring of an evolving fuel spray. The primary emission is in the green, and frequency doubling would be required in order to pump systems in the ultraviolet. The beam quality is generally poor.

b. Detectors

As with excitation lasers, there is not a unique choice of detector, and the considerations in this section are intended as a modest guide.

Sensitivity in the Ultraviolet

No detector is of any use if the optics preceding it absorb all the light. Be sure that the detector can be fitted with optics which do not absorb appreciably in the region to be studied. TMPD emits at approximately 390 nm, and the anti-reflection coatings in a standard "zoom lens" already absorb approximately 90% of the light at this wavelength. Similarly, quartz windows should be specified on the photodetectors instead of glass since this will help alleviate the need for the use of scintillator coatings, which generally have low sensitivity. The vaporization systems under development for the more volatile fuels will produce fluorescence in the 250-350 nm region, and detector choices should be made with this in mind.

Photographic Film

Film is not the optimal detector --linearity and speed of data processing are problems -- but it should not be forgotten either. High speed films are fast enough to take photographs of a spray with a single pulse of a Nd:YAG laser, and thus "stopped action" photographs can be obtained.

Television Cameras

Television cameras, or vidicons, can be used to obtain computer processable images of evaporating sprays. Vapor intensity is generally a problem, and intensified cameras are generally necessary. The low framing rate does not allow real-time studies of fuel sprays, and multiple reads may be necessary to clear the accumulated charge. Linearity is generally good.[26,27]

Diode Array Detectors

These detectors can provide fast, linear response with a wide dynamic range, and the data is readily computer processable. Intensified detectors are generally necessary. The data transfer rates may limit the use in real-time studies.[26,27]

2. Visualization Studies by M .E. A. Bardsley, P. G. Felton, and F. V. Bracco Princeton University[29]

The above-listed authors have prepared a paper [2-D Visualization of Liquid and Vapor Fuel in an I. C. Engine] in which they describe the application of these exciplex-based vapor/liquid visualization systems to qualitative studies of fuel spray evolution in the combustion chamber of a single cylinder, direct injection internal combustion engine. Because of the strong quenching of the vapor phase fluorescence by oxygen, the data are reported for a motored engine using nitrogen rather than air.

In the process of applying the exciplex-based visualization systems, Bardsley et al. have identified some of the elements of a working visualization apparatus. Their system is briefly summarized here; the paper provides a more complete description. The laser used was a frequency-tripled Quanta-Ray DCR-1A Nd:YAG operated at five pulses/sec. The third harmonic of the Nd:Yag laser (355 nm) was used in order to obtain a more nearly optically thin system. The fluorescent emissions were collected at 90 degrees to the laser sheet. A Reticon MC-521 camera (100 x 100 pixels) with an ITT F4144 microchannel plate intensifier capable of luminous gain of 10^4, interfaced via a Reticon RS-521 controller, was used to acquire images. The exciplex signal (liquid phase) was isolated with a Melles-Griot 03LWP001 filter (long wavelength passing > 450 nm), and the monomer signal (vapor phase) was isolated with a Corion broad band interference filter centered at 400 nm with a FWHM of 25 nm.

VI. Estimation of Limiting Accuracy

In using any quantitative method, it is necessary to have estimates of the accuracy with which the derived

quantities may be determined. In terms of the exciplex-based vapor/liquid visualization systems, if the signal intensities $S_f(x,y,z_o,L_E,DL)$ and $S_f(x,y,z_o,L_M,DL)$ are measured accurately ($\pm$ 1% for example), what estimates of accuracy are appropriate for the derived values $M_l(x,y,z_o)$ and $M_v(x,y,z_o)$? Examination of the detailed equations (12a) and (12b) shows that the functions can be separated into two classes: 1) functions which can be determined with accuracy of 1-5% [$\langle F*H\rangle_l(T_o,C_{l\,o},n,',f\#)$, $H_v(f\#)$, $A_E(L)$, $A_M(L)$, $G_l(T_o,C_{l\,o},L)$, and $G_v(T_o,C_{v\,o},L)$], and 2) functions which may have uncertainties of > 15% [$Q_{f-l}(T_o,C_{l\,o})$, $F_{***-v}(T_o,C_{v\,o},L_{**})$, and $Q_{f-v}(T_o,C_v)$]. In addition, there is the problem of overlap of signals, which will be particularly troublesome when a weak vapor phase signal is to be measured in the presence of a strong liquid phase signal (which necessarily emits in the "vapor phase" spectral region). For a given vapor/liquid visualization system, this last problem is fundamentally one which can be resolved only by obtaining a higher signal-to-noise ratio in the intensity measurements. The errors introduced by the functions with large uncertainties are systematic errors arising from limitations of the exciplex-based visualization method, and these errors require further examination.

$Q_{f-l}(T_o,C_{l\,o})$

Two sources of error enter the estimation of $Q_{f-l}(T_*,C_{l\,*})$: the 13% random error in the determination of the quantum yield at room temperature and the error due to the decrease of the quantum yield with temperature. As the spray evolves, droplets will have different temperatures, and yet the method requires the assumption that the temperature does not affect the sensitivity to liquid phase mass. Since the fall in the quantum yield is about 30% at 250 C, one can pick an intermediate value and argue that the absolute error is no more than $\pm$ 15%, i.e., half of 30%. The root-mean-square estimated error is then about $\pm$ 20%.

$F_{***-v}(T_o,C_{v\,o},L_{**})$

All the quantities involved in calculating $F_{***-v}(T_o,C_{v\,o},L_{**})$ can be determined accurately except $C_v'(M)$, the mass fraction of the marker in the vapor (M, G, and F only). The equilibrium distillation calculations shown in figures 11 and 12 indicate that the 1 TMPD/10 N/89 T and 1 TMPD/10 1M-N/89 T systems should have a maximum deviation of -20% and -12% from the ideal value, C_l, respectively. Again one can pick an intermediate value, use a corrected value for $C_v'(M)$ [= (1 - 0.5 * abs(maximum fractional deviation)], and assign an estimated error of half the maximum deviation. In this case those estimated errors would be 10% and 6%, respectively.

$Q_{f-v}(T_s, C_v)$

Two sources of error enter into the calculation of $Q_{f-v}(T_s, C_v)$: 1) The value of the absolute quantum yield for vapor phase TMPD fluorescence has not been measured, and 2) since quenching by molecular oxygen is very efficient, unknown amounts of oxygen mixed into the vapor will cause large uncertainties in $Q_{f-v}(Ts, C_v)$. The first problem can be resolved with further experimental work, and given the estimated value of $Q_{f-v}(TMPD)$, the measured value will probably have an estimated uncertainty of approximately $\pm$ 15%. At present, the only way to deal with the second problem is to require that the system be purged of oxygen, in the liquid and in the vapor.

The aggregate root-mean-square error for these three sources is approximately $\pm$ 25%. The contributions from the several smaller sources of error are not expected to increase this figure significantly.

Direct calibration techniques do not remove the problem of systematic errors. In the liquid phase, direct calibration techniques are not presently available for a full spray, and it is hard to imagine that such a technique could truly remove the ambiguity introduced by the confounding of a temperature-dependent liquid phase quantum yield with the evolving temperature distribution in the fuel spray. In the vapor phase, where an excellent direct calibration technique is available,[13] such a calibration would still not remove the ambiguity caused by the uncertain ratio of the marker M to the total fuel mass (M, G, and F) in the vapor.

VII. Updating of Users Manual

A. Two Way Communications

This users manual is intended to provide the engineering community with a comprehensive summary of the photophysical functions/parameters underlying the two exciplex-based vapor/liquid visualization systems which are furthest along in the development/characterization process. In preparing this document, it has become clear that anticipation of every important/confusing detail is impossible, and therefore questions and suggestions for revisions/additions are solicited. A modest attempt will be made to maintain a mailing list of users, and to that end, it is requested that users write to the author periodically to provide new questions and suggestions, to convey technology which makes the visualization systems more viable, to request updates to the manual, and to solicit advice on the problems involved in adapting the visualization systems to realistic applications. The address for correspondence is as follows:

Dr. Lynn A. Melton
Department of Chemistry
University of Texas at Dallas
Box 830688
Richardson, TX 75083
(214/690-2901)

B. Information to come

This manual has summarized the work of many experiments, most of which are sufficiently complete to report their results with confidence, but which have not yet been submitted for publication. A summary of the subjects of these papers is provided below:

1. Absorption and Fluorescence Efficiencies in Droplets

2. Five Exciplex-Based Vapor/Liquid Visualization Systems for Diesel/Gas Turbine Fuels

3. Measurement of the Absolute Quantum Yield for Selected Exciplex Fluorescence as a Function of Temperature

4. Adaptation of Exciplex-Based Vapor/Liquid Visualization Systems for Use with Real Fuels

5. Direct Calibration Methods for Use with Exciplex-Based Vapor/Liquid Visualization Systems

6. Exciplex-Based Vapor/Liquid Visualization Systems for Fuels Boiling in the Range 0-150 C

7. Extension of the Rehm and Weller Analysis to Amine-Based Exciplexes

VIII. Acknowledgements

This manual was prepared under Army Research Office contract DAAL03-86-K-0082. It also incorporates results obtained under AFOSR grant 83-0307 and ARO contract DAAG29-84-C-0010. Dr. David Mann of ARO and Dr. Julian Tishkoff of AFOSR have provided continued encouragement during these projects. Their combined support and encouragement is gratefully acknowledged. Dr. Alice M. Murray, Dr. Thomas D. Padrick (post-doctoral research associates), Stanley K. Nickle, Stephanie Hale (graduate students), Jerry Hogan (undergraduate research student), Marilyn Huff, and Kristin Hahn (Clark Foundation Research Students) have carried out much of the experimental and computational work.

REFERENCES

1. L. A. Melton, "Fluorescent Additives for the Determination of Condensed and Vapor Phases in Multiphase Systems," U. S. Patent 4,515,896; issued May 7, 1985; assigned to United Technologies Corporation.

2. L. A. Melton, "Spectrally Separated Fluorescence Emissions for Diesel Fuel Droplets and Vapor," Appl. Opt., 22, 2224 (1983).

3. L. A. Melton and J. F. Verdieck, "Vapor/Liquid Visualization for Fuel Sprays," Combustion Sci. and Tech., 42, 217 (1984).

4. L. A. Melton and J. F. Verdieck, "Vapor/Liquid Visualization in Fuel Sprays," in Proceedings, XXth Symposium (International) on Combustion (The Combustion Institute), Pittsburgh, 1984), 1283.

5. L. A. Melton, A. M. Murray, and J. F. Verdieck, "Laser Fluorescence Measurements for Fuel Sprays," in SPIE Symposium Series, Remote Sensing - 644, 40 (1986).

6. T. Forster, "Excimers," Angew. Chem. Int. Ed., 8, 333 (1969).

7. D. Rehm and A. Weller, "Bound States and Fluorescence of Heteroexcimers," Z. Phys. Chem. (Frankfurt am Main), 69, 183 (1970).

8. J. B. Birks, "Excimer Fluorescence in Organic Compounds," in Progress in Reaction Kinetics, G. Porter, Ed., 5, (Pergamon, London, 1969).

9. L. A. Melton, "Method for Determining the Temperature of a Fluid," U. S. Patent 4,613,237; issued September 23, 1986; assigned to United Technologies Corporation.

10. A. M. Murray and L. A. Melton, "Fluorescence Methods for Determination of Temperature in Fuel Sprays," Appl. Opt., 24, 2783 (1984).

11. H. E. Gossage and L. A. Melton, "Fluorescence Thermometers Using Intramolecular Exciplexes", Appl Opt., 26, 2256 (1987).

12. J. F. Owen, R. K. Chang, and P. W. Barber, "Morphology-Dependent Resonances in Raman Scattering, Fluorescence Emission, and Elastic Scattering from Microparticles," Aerosol Sci. and Tech., 1, 293 (1984).

13. D. S. Benincasa, P. W. Barber, J-Z Zhang, W-F Hsieh, and R. K. Chang, "Spatial Distribution of the Internal and Near-Field Intensities of Large Cylindrical and Spherical Scatterers," Appl. Opt., 26, 1348 (1987).

14. S. Hale, "Quantum Yield Measurements of Exciplexes," Apprenticeship Practicum Report, Department of Chemistry, University of Texas at Dallas, July 1987.

15. A. M. Murray, T. D. Padrick, and L. A. Melton, unpublished data.

16. S. K. Nickle, "Vapor Phase Quenching of Fluorescence of Organic Molecules," Fundamental Practicum Report, Department of Chemistry, University of Texas at Dallas (1987).

17. N. J. Turro, Modern Molecular Photochemistry, (Benjamin-Cummings, Menlo Park, 1978).

18. Landolt-Bornstein Zahlenwerte und Funktionen, Sechste Auflage, II. Band, 8. Teil (Optische Konstanten), (Springer-Verlag, Berlin, 1962), pp 5-631, 5-585, 5-586.

19. I. B. Berlman, Handbook of Fluorescence Spectra of Aromatic Molecules (Academic, New York, 1971).

20. M. E. A. Bardsley, P. G. Felton, and F. V. Bracco, "2-D Visualization of Liquid and Vapor Fuel in an I. C. Engine", to be presented at the SAE 1988 International Congress (Detroit, February 1988).

21. A. Y. Tong and W. A. Sirignano, "Multicomponent Droplet Vaporization in a High Temperature Gas," Combust. Flame, 66, 221 (1986).

22. L. A. Melton and Q-Z Lu, unpublished data.

23. A. J. Gordon and R. A. Ford, The Chemist's Companion: A Handbook of Practical Data, Techniques, and References (Wiley, New York, 1972), p. 435.

24. Aldrich Chemical Co., Catalog/Handbook of Fine Chemicals 1986-87.

25. A. L. Randolph and C. K. Law, "Influence of Physical Mechanisms on Soot Formation and Destruction in Droplet Burning," Combust. Flame, 64, 267 (1986).

26. B. Yip, J. K. Lam, M. Winter, and M. B. Long, "Time-Resolved Three-Dimensional Concentration Measurements in a Gas Jet," Science, 235, 1209 (1987).

27. M. Winter, J. K. Lam, and M. B. Long, "Techniques for High-Speed Digital Imaging of Gas Concentrations in Turbulent Flows," Experiments in Fluids, 5, 177 (1987).

SYMBOL TABLE

Chemical Species and Chemicals

M	monomer in the exciplex, used as the marker for the vapor; M* is the first excited state of M;
G	ground state reactant in the exciplex;
F	fuel, or more generally, the (non-photoactive) solvent;
E*	exciplex;
TMPD	N,N,N',N'-tetramethyl-p-phenylenediamine;
N	naphthalene;
1MN	1-methylnaphthalene;
T	n-tetradecane;
H	n-hexadecane;

Algebraic Quantities

a	coefficient in equation (28);
A	radiative rate constant;
A(L)	spectral response function;
$A_E(L)$	spectral response function for isolation of exciplex emission;
$A_M(l)$	spectral response function for isolation of monomer emission;
b	coefficient in equation (28);
b'	coefficient in equation (25);
B_l	coefficients in equations (13a) and (13b);
B_v	coefficients in equations (13a) and (13b);
C_l	mass fraction composition of liquid;
C_v	mass fraction composition of vapor;
C_v'	C_v computed using only M, G, and F;
d_l	density of liquid phase;
DL	wavelength interval;
Dx,Dy,Dz	intervals of the coordinates;
f#	aperture of collecting lens;
$\langle F*H \rangle_l$	integral over F and H for droplets;
F'_{abs-l}	fraction of light absorbed in liquid;
F'_{abs-v}	fraction of light absorbed in vapor;
F_{corr-l}	corrected fluorescence spectrum of liquid;
F_{corr-v}	corrected fluorescence spectrum of vapor;
G_l	spectral yield function for the liquid;
G_v	spectral yield function for the vapor;
H_l	fraction of light emitted into lens aperture by liquid;
Hv	fraction of light emitted into lens aperture by vapor;
I	intensity of laser;
J	index for components in equation (24);
k	coefficient in equation (4);
k'	slope of figure 4b;

$K_q(i)$	rate constant for the quenching of M* by i;
K_i	sum of rate constants for internal conversion and intersystem crossing for M*;
L	wavelength;
L_E	wavelength at which exciplex emission is detected;
L_M	wavelength at which monomer emission is detected;
L_{ex}	excitation wavelength;
L_{max}	wavelength of maximum fluorescence emission;
M_{di}	mass of droplet i;
$M_{droplet}$	mass of droplets;
M_l	mass of liquid in voxel;
m_l	mass concentration of liquid in voxel;
M_v	mass of vapor in voxel;
MW	molecular weight;
m_v	mass concentration of vapor in voxel;
n	index of refraction of liquid;
N_l	number of photons emitted by droplet into lens aperture;
N_v	number of photons emitted by voxel of vapor into lens aperture;
P_i	pressure of component i;
P_M	pressure of M;
Q'_{f-l}	fraction of liquid emission into wavelength interval;
Q_{f-l}	absolute quantum yield of liquid;
Q'f-v	fraction of vapor emission into wavelength interval;
Q_{f-v}	absolute quantum yield of vapor;
r_i	radius of droplet i;
r_l	calibration constant for liquid in equation (29);
r_v	calibration constant for vapor in equation(30);
S_f	fluorescence signal;
S_{fl}	fluorescence signal from liquid;
S_{fv}	fluorescence signal from vapor;
T	temperature;
X,Y,Z	coordinate system;
x,y,z	coordinates within the spray;
x_d, y_d, z_d	coordinates within a droplet;
x'	variable in equation (28);
z_o	coordinate of laser sheet;

Subscripts

abs	absorption;
atm	pressure in atmospheres;
corr	corrected spectrum;
d	droplet;
f	fluorescence
l	liquid;
v	vapor;
o	time-independent value;
E	exciplex;
M	monomer;

Greek Characters

ε	molar absorptivity;
ε'	mass absorptivity;
ν	photon energy in wavenumbers;
τ	lifetime of excited TMPD;

TABLE I

$k'(T, C_1, n, f\#)$

f#	n		
	1.35	1.40	1.45
3.5	0.0059	0.0057	0.0055
6	0.0017	0.00165	0.00155
10	0.0004	0.0004	0.00035

Table II

Vapor Phase Absorbance of TMPD
T = 175 - 275 °C

L(nm)	ε(liter/mole-cm)
290	2670 ± 70
300	2025 ± 18
310	1796 ± 21
320	1548 ± 26
330	1196 ± 10
340	726 ± 10
350	315 ± 10

Table III

Selected Values of Index of Refraction[10]

molecule	L(nm)	n
$C_{16}H_{34}$ n-hexadecane	656	1.43242
	486	1.44002
	434	1.44451
C14H30 n-tetradecane	656	1.4269
	486	1.4343
	434	1.4382
$C_{12}H_{26}$ n-dodecane	656	1.4197
	486	1.4272
	434	not available
C6H12 cyclohexane	656	1.4241
	486	1.4319
	436	1.4362

All values at 20 °C

Figure Captions

1. Exciplex Energy Level Diagram

2. Vapor/Liquid Visualization Concept for Exciplex-Based Systems

3. Coordinate System for Visualization Equations

4. Fraction of Light Incident on a Droplet which is Refracted into Droplet, Absorbed, and Emitted into Lens Aperture as a Function of Droplet Optical Density (D.O.D.): a) log-log plot, b) linear plot.

5. TMPD-Naphalene Exciplex Emission Spectra (spectrally corrected, normalized to set maximum = 1.00): a) T = 24 °C, b) T = 65 °C, c) T = 94 °C, d) T = 138 °C, e) T = 156 °C, f) T = 172 °C, g) T = 206 °C, h) T = 221 °C, i) T = 259 °C. High frequency pattern shown on some spectra is an instrumental effect.

6. TMPD Emission Spectrum (vapor, spectrally corrected, normalized to set maximum = 1.00).

7. Absolute Quantum Yield of TMPD-Naphthalene Exciplex as a Function of Temperature.

8. Absorbance Spectrum of Naphthalene.

9. Absorbance Spectrum of 1-Methylnaphthalene.

10. Absorbance Spectrum of TMPD.

11. Percentage of Vapor Phase Marker Evaporated as a Function of Percentage of Droplet Evaporated, 1 TMPD/10 N/ 89 T. Diagonal Represents Ideal Behavior.

12. Percentage of Vapor Phase Marker Evaporated as a Function of Perecentage of Droplet Evaporated, 1 TMPD/10 1MN/89 T. Diagonal Represents Ideal Behavior.

EXCIPLEX ENERGY LEVEL DIAGRAM

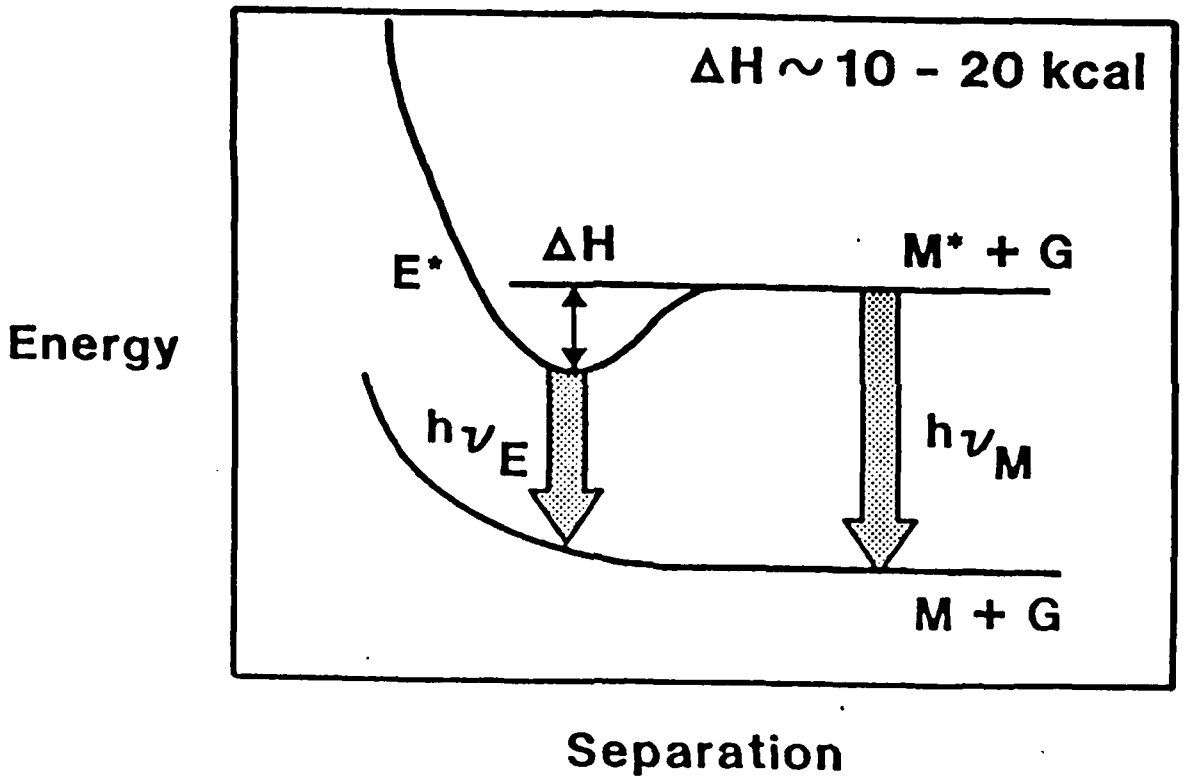

86-10-72-25

RE848TX.001

REAL TIME, 2-D SPRAY/VAPOR MONITORING VIA EXCIPLEX FLUORESCENCE

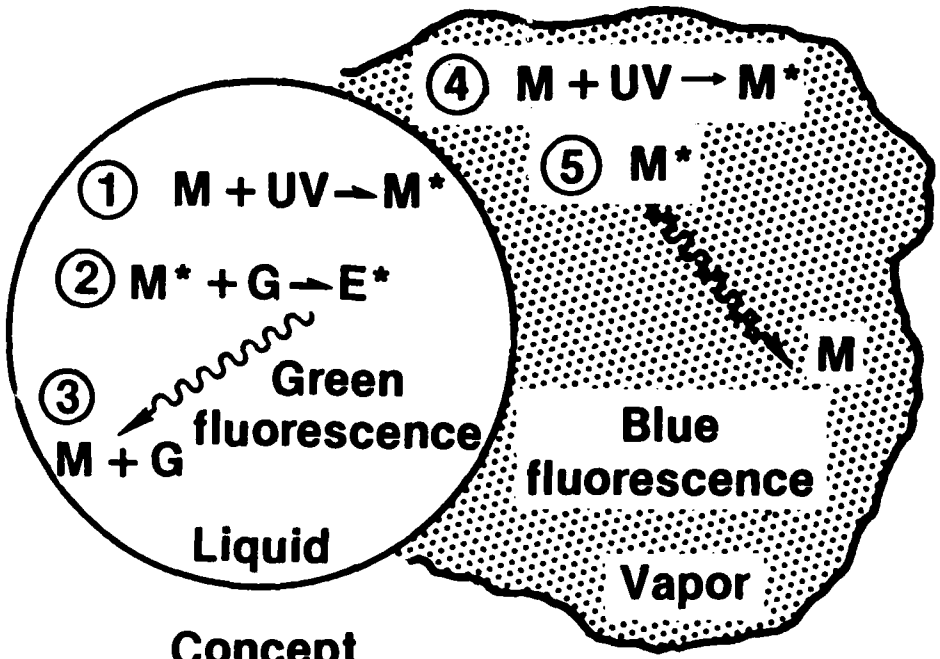

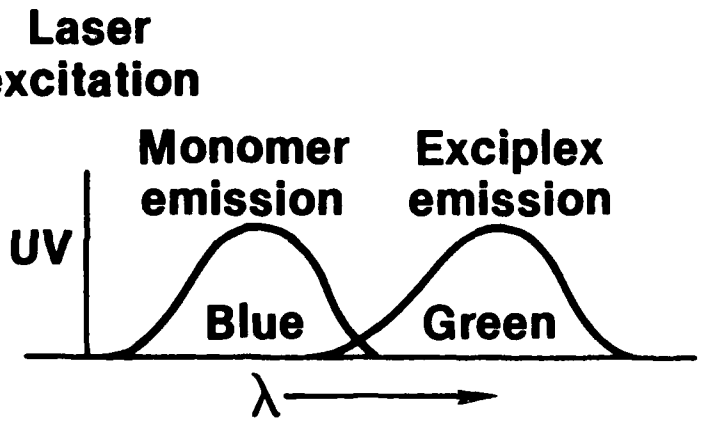

Concept

① , ④ Laser excitation of monomer in liquid or vapor

② Exciplex (excited complex) formation, liquid phase only

③ Exciplex fluorescence occurs in green

⑤ Monomer fluorescence occurs in blue

83-2-23-3

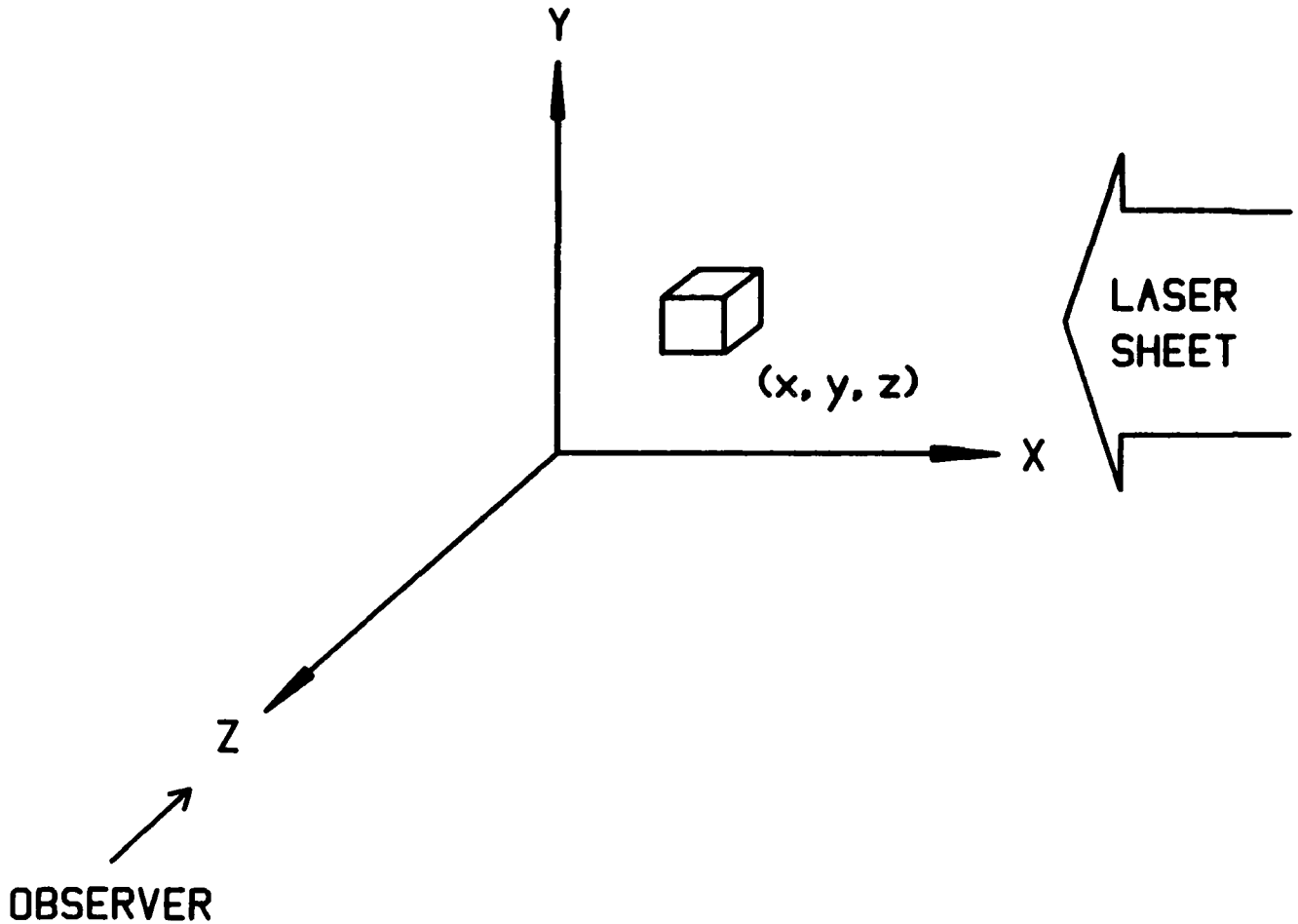

Fig. 3

Fig. 4a

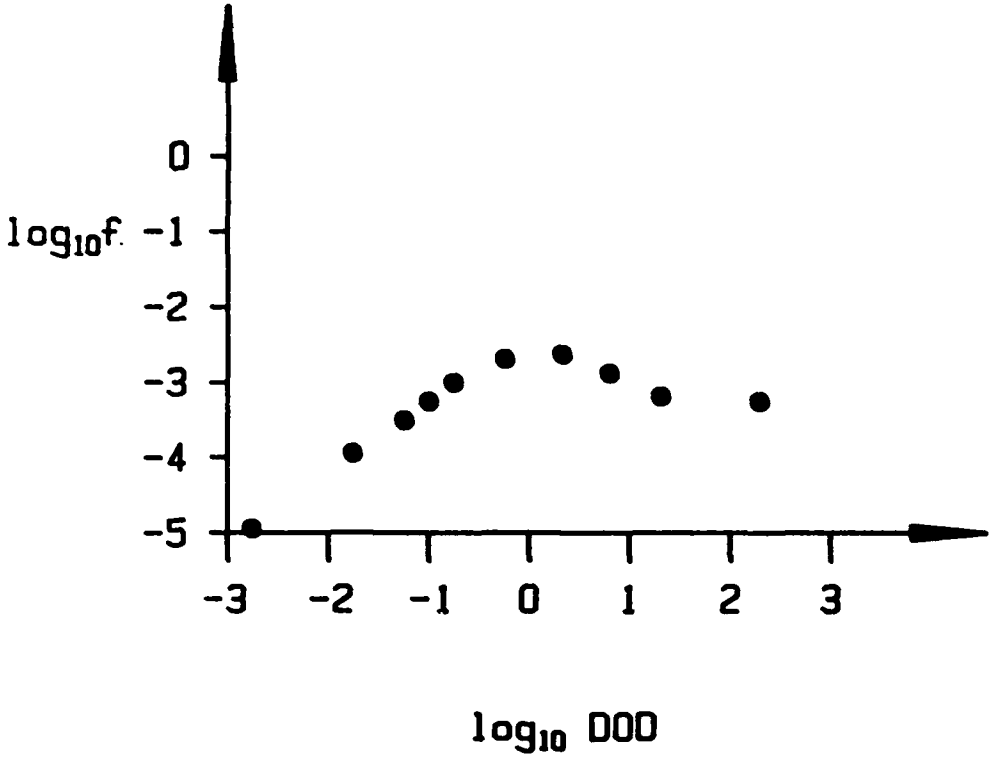

Fig. 4b

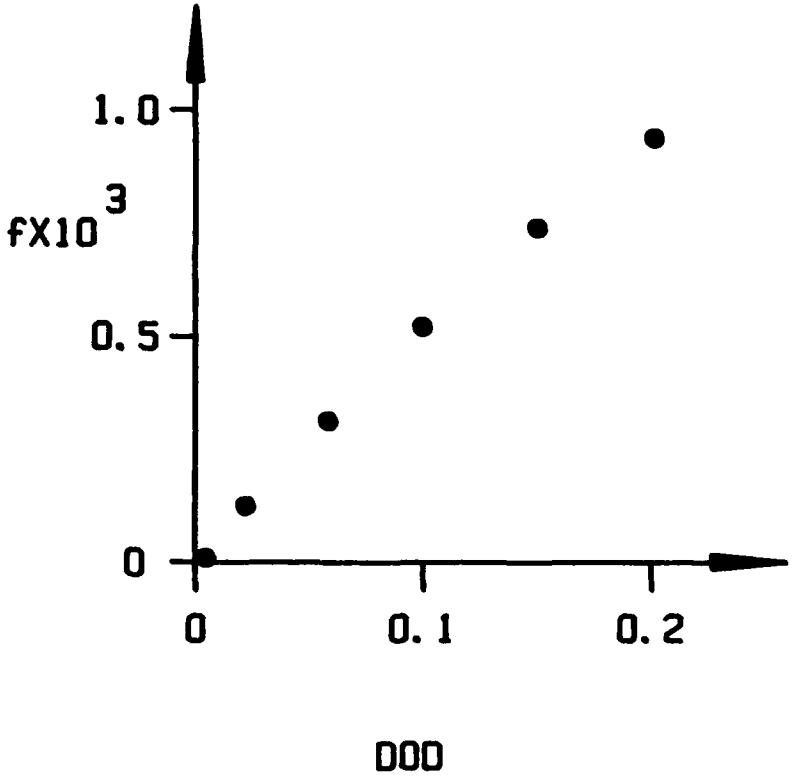

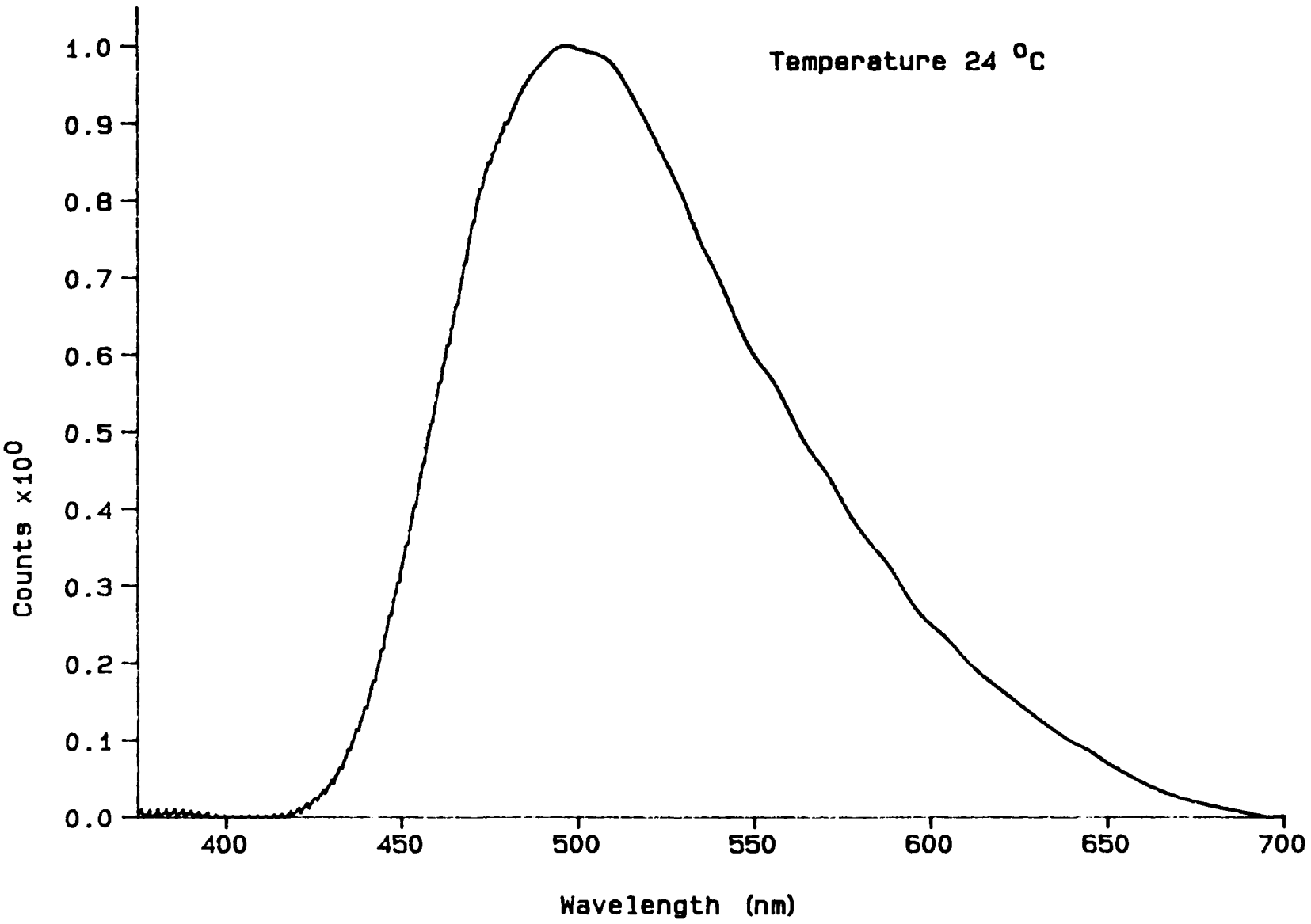
TMPD-Napthalene Exciplex Emission
Temperature 24 °C
Counts x10^0
1.0
0.9
0.8
0.7
0.6
0.5
0.4
0.3
0.2
0.1
0.0
400
450
500
550
600
650
700
Wavelength (nm)

SPECTRAL YIELD FUNCTION FOR SPECTRUM 5A

TMPD-Napthalene Exciplex

Wavelength	Intensity	Wavelength	Intensity	Wavelength	Intensity
417.1	2.241E-05	525.0	4.367E-03	632.9	6.028E-04
419.4	3.862E-05	527.3	4.253E-03	635.2	5.638E-04
421.8	7.183E-05	529.7	4.126E-03	637.6	5.274E-04
424.1	1.130E-04	532.0	3.984E-03	639.9	4.950E-04
426.5	1.560E-04	534.4	3.847E-03	642.3	4.657E-04
428.8	2.168E-04	536.7	3.731E-03	644.6	4.340E-04
431.2	2.946E-04	539.1	3.620E-03	647.0	3.963E-04
433.5	4.069E-04	541.4	3.494E-03	649.3	3.578E-04
435.9	5.394E-04	543.7	3.359E-03	651.6	3.239E-04
438.2	6.846E-04	546.1	3.233E-03	654.0	2.934E-04
440.5	8.525E-04	548.4	3.126E-03	656.3	2.634E-04
442.9	1.041E-03	550.8	3.045E-03	658.7	2.342E-04
445.2	1.271E-03	553.1	2.976E-03	661.0	2.073E-04
447.6	1.499E-03	555.5	2.892E-03	663.4	1.831E-04
449.9	1.741E-03	557.8	2.785E-03	665.7	1.615E-04
452.3	2.001E-03	560.2	2.670E-03	668.1	1.421E-04
454.6	2.273E-03	562.5	2.558E-03	670.4	1.248E-04
457.0	2.552E-03	564.9	2.464E-03	672.8	1.091E-04
459.3	2.830E-03	567.2	2.390E-03	675.1	9.497E-05
461.7	3.082E-03	569.5	2.314E-03	677.4	8.196E-05
464.0	3.344E-03	571.9	2.219E-03	679.8	6.987E-05
466.3	3.611E-03	574.2	2.116E-03	682.1	5.844E-05
468.7	3.883E-03	576.6	2.020E-03	684.5	4.739E-05
471.0	4.147E-03	578.9	1.935E-03	686.8	3.647E-05
473.4	4.335E-03	581.3	1.863E-03	689.2	2.540E-05
475.7	4.474E-03	583.6	1.796E-03	691.5	1.392E-05
478.1	4.606E-03	586.0	1.728E-03	693.9	1.766E-06
480.4	4.719E-03	588.3	1.652E-03	696.2	1.133E-05
482.8	4.849E-03	590.7	1.564E-03	698.6	2.564E-05
485.1	4.947E-03	593.0	1.470E-03		
487.5	5.023E-03	595.4	1.388E-03		
489.8	5.088E-03	597.7	1.325E-03		
492.1	5.143E-03	600.0	1.275E-03		
494.5	5.176E-03	602.4	1.226E-03		
496.8	5.174E-03	604.7	1.173E-03		
499.2	5.156E-03	607.1	1.109E-03		
501.5	5.140E-03	609.4	1.046E-03		
503.9	5.126E-03	611.8	9.914E-04		
506.2	5.103E-03	614.1	9.441E-04		
508.6	5.062E-03	616.5	9.003E-04		
510.9	4.994E-03	618.8	8.577E-04		
513.3	4.902E-03	621.2	8.149E-04		
515.6	4.801E-03	623.5	7.717E-04		
517.9	4.698E-03	625.8	7.284E-04		
520.3	4.591E-03	628.2	6.855E-04		
522.6	4.479E-03	630.5	6.435E-04		

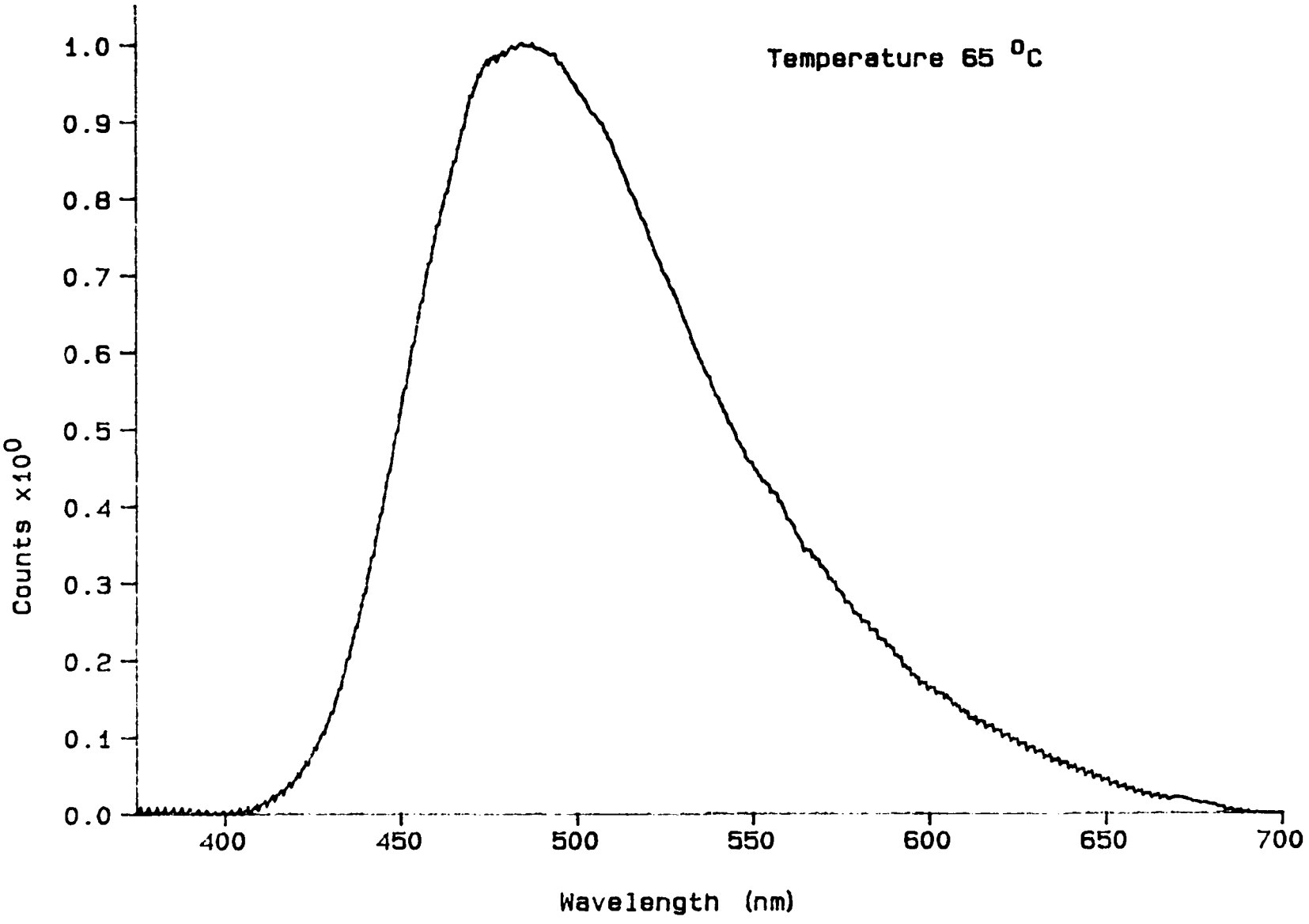
TMPD-Napthalene Exciplex Emission
Temperature 65 °C
Counts x10⁰
1.0
0.9
0.8
0.7
0.6
0.5
0.4
0.3
0.2
0.1
0.0
400
450
500
550
600
650
700
Wavelength (nm)

SPECTRAL YIELD FUNCTION FOR SPECTRUM 5B

TMPD-Napthalene Exciplex

Wavelength	Intensity	Wavelength	Intensity	Wavelength	Intensity
405.4	2.944E-05	513.3	4.544E-03	621.2	5.608E-04
407.7	4.702E-05	515.6	4.404E-03	623.5	5.312E-04
410.1	7.979E-05	517.9	4.246E-03	625.8	< 4.971E-04
412.4	1.087E-04	520.3	4.097E-03	628.2	4.695E-04
414.7	1.461E-04	522.6	3.956E-03	630.5	4.378E-04
417.1	1.959E-04	525.0	3.828E-03	632.9	4.055E-04
419.4	2.517E-04	527.3	3.700E-03	635.2	3.753E-04
421.8	3.347E-04	529.7	3.545E-03	637.6	3.555E-04
424.1	4.242E-04	532.0	3.390E-03	639.9	3.239E-04
426.5	5.432E-04	534.4	3.247E-03	642.3	3.118E-04
428.8	6.670E-04	536.7	3.117E-03	644.6	2.881E-04
431.2	8.279E-04	539.1	2.979E-03	647.0	2.617E-04
433.5	1.032E-03	541.4	2.864E-03	649.3	2.417E-04
435.9	1.258E-03	543.7	2.740E-03	651.6	2.154E-04
438.2	1.486E-03	546.1	2.609E-03	654.0	1.949E-04
440.5	1.747E-03	548.4	2.501E-03	656.3	1.738E-04
442.9	2.035E-03	550.8	2.415E-03	658.7	1.531E-04
445.2	2.331E-03	553.1	2.348E-03	661.0	1.372E-04
447.6	2.634E-03	555.5	2.282E-03	663.4	1.218E-04
449.9	2.933E-03	557.8	2.181E-03	665.7	1.132E-04
452.3	3.233E-03	560.2	2.068E-03	668.1	1.071E-04
454.6	3.544E-03	562.5	1.952E-03	670.4	1.102E-04
457.0	3.847E-03	564.9	1.871E-03	672.8	9.472E-05
459.3	4.112E-03	567.2	1.807E-03	675.1	8.290E-05
461.7	4.347E-03	569.5	1.738E-03	677.4	7.217E-05
464.0	4.575E-03	571.9	1.653E-03	679.8	5.988E-05
466.3	4.798E-03	574.2	1.573E-03	682.1	4.207E-05
468.7	5.044E-03	576.6	1.502E-03	684.5	2.824E-05
471.0	5.211E-03	578.9	1.415E-03	686.8	2.279E-05
473.4	5.341E-03	581.3	1.363E-03	689.2	1.235E-05
475.7	5.387E-03	583.6	1.306E-03	691.5	8.187E-07
478.1	5.420E-03	586.0	1.236E-03	693.9	1.010E-05
480.4	5.464E-03	588.3	1.184E-03	696.2	2.160E-05
482.8	5.475E-03	590.7	1.113E-03	698.6	2.960E-05
485.1	5.481E-03	593.0	1.033E-03		
487.5	5.468E-03	595.4	9.753E-04		
489.8	5.450E-03	597.7	9.285E-04		
492.1	5.411E-03	600.0	8.991E-04		
494.5	5.348E-03	602.4	8.564E-04		
496.8	5.281E-03	604.7	8.191E-04		
499.2	5.184E-03	607.1	7.664E-04		
501.5	5.097E-03	609.4	7.204E-04		
503.9	4.995E-03	611.8	6.693E-04		
506.2	4.927E-03	614.1	6.601E-04		
508.6	4.814E-03	616.5	6.212E-04		
510.9	4.684E-03	618.8	5.931E-04		

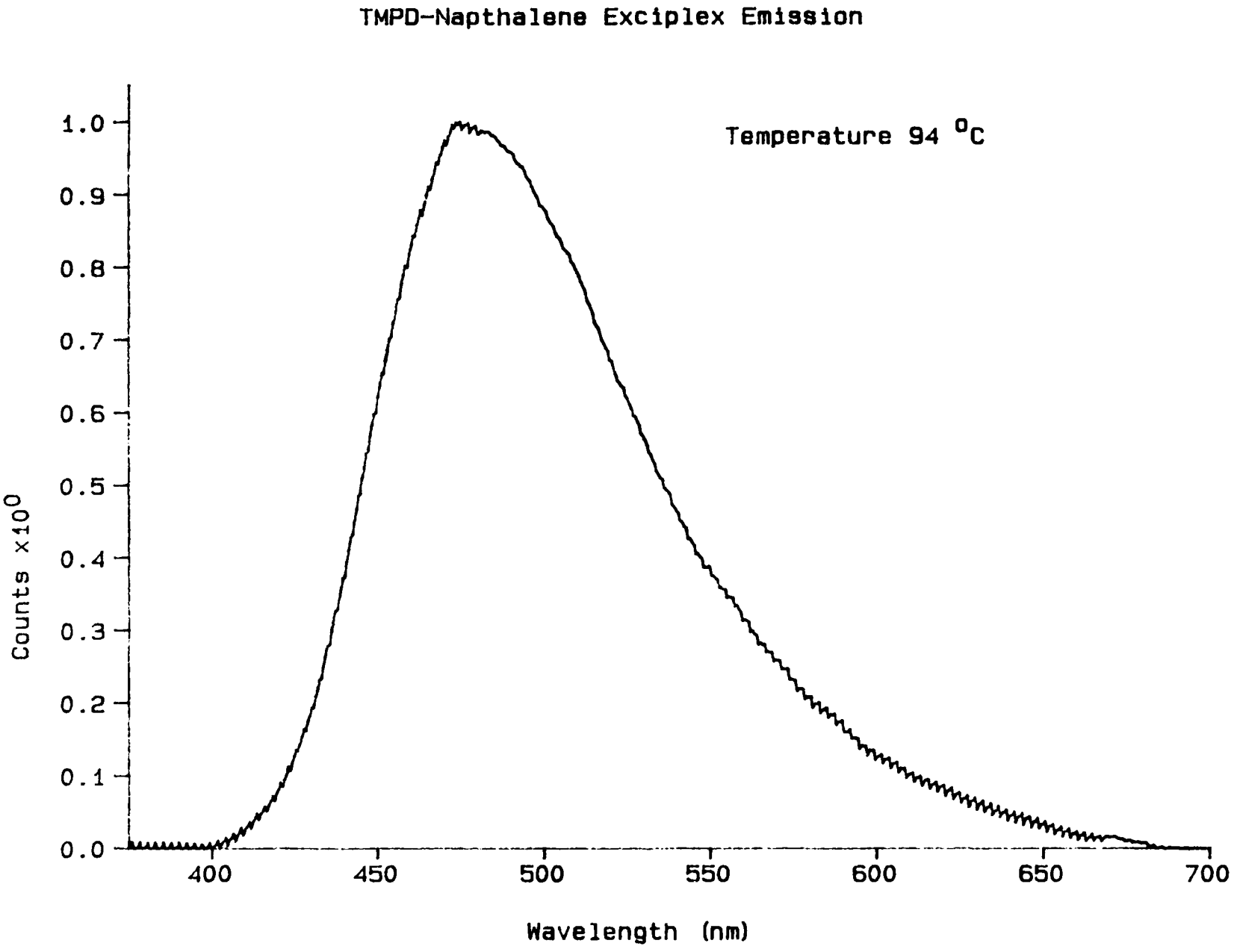
TMPD-Napthalene Exciplex Emission
Temperature 94 °C
Counts x10^0
1.0
0.9
0.8
0.7
0.6
0.5
0.4
0.3
0.2
0.1
0.0
400
450
500
550
600
650
700
Wavelength (nm)

SPECTRAL YIELD FUNCTION SPECTRUM 5C

TMPD-Napthalene Exciplex

Wavelength	Intensity	Wavelength	Intensity	Wavelength	Intensity
400.7	2.969E-05	508.6	4.576E-03	616.5	5.074E-04
403.0	5.735E-05	510.9	4.435E-03	618.8	4.916E-04
405.4	8.438E-05	513.3	4.269E-03	621.2	4.587E-04
407.7	1.231E-04	515.6	4.107E-03	623.5	4.322E-04
410.1	1.753E-04	517.9	3.946E-03	625.8	3.951E-04
412.4	2.390E-04	520.3	3.787E-03	628.2	3.788E-04
414.7	2.960E-04	522.6	3.646E-03	630.5	3.553E-04
417.1	3.749E-04	525.0	3.507E-03	632.9	3.267E-04
419.4	4.703E-04	527.3	3.366E-03	635.2	3.007E-04
421.8	5.845E-04	529.7	3.219E-03	637.6	2.826E-04
424.1	7.244E-04	532.0	3.063E-03	639.9	2.621E-04
426.5	8.819E-04	534.4	2.920E-03	642.3	2.548E-04
428.8	1.044E-03	536.7	2.807E-03	644.6	2.359E-04
431.2	1.249E-03	539.1	2.667E-03	647.0	2.106E-04
433.5	1.508E-03	541.4	2.543E-03	649.3	1.887E-04
435.9	1.783E-03	543.7	2.416E-03	651.6	1.734E-04
438.2	2.048E-03	546.1	2.300E-03	654.0	1.467E-04
440.5	2.353E-03	548.4	2.220E-03	656.3	1.354E-04
442.9	2.678E-03	550.8	2.128E-03	658.7	1.141E-04
445.2	3.009E-03	553.1	2.045E-03	661.0	1.051E-04
447.6	3.334E-03	555.5	1.979E-03	663.4	9.031E-05
449.9	3.651E-03	557.8	1.887E-03	665.7	9.020E-05
452.3	3.929E-03	560.2	1.797E-03	668.1	9.074E-05
454.6	4.235E-03	562.5	1.688E-03	670.4	9.134E-05
457.0	4.520E-03	564.9	1.604E-03	672.8	7.024E-05
459.3	4.755E-03	567.2	1.543E-03	675.1	6.203E-05
461.7	4.972E-03	569.5	1.480E-03	677.4	5.363E-05
464.0	5.151E-03	571.9	1.413E-03	679.8	4.249E-05
466.3	5.338E-03	574.2	1.326E-03	682.1	2.321E-05
468.7	5.536E-03	576.6	1.258E-03	684.5	9.614E-06
471.0	5.651E-03	578.9	1.190E-03	686.8	7.032E-06
473.4	5.713E-03	581.3	1.139E-03	689.2	6.780E-06
475.7	5.712E-03	583.6	1.091E-03	691.5	1.708E-05
478.1	5.690E-03	586.0	1.052E-03	693.9	2.369E-05
480.4	5.670E-03	588.3	1.000E-03	696.2	3.584E-05
482.8	5.650E-03	590.7	9.172E-04	698.6	4.295E-05
485.1	5.587E-03	593.0	8.642E-04		
487.5	5.533E-03	595.4	8.045E-04		
489.8	5.479E-03	597.7	7.715E-04		
492.1	5.379E-03	600.0	7.290E-04		
494.5	5.283E-03	602.4	7.052E-04		
496.8	5.156E-03	604.7	6.759E-04		
499.2	5.049E-03	607.1	6.231E-04		
501.5	4.924E-03	609.4	5.870E-04		
503.9	4.815E-03	611.8	5.571E-04		
506.2	4.701E-03	614.1	5.413E-04		

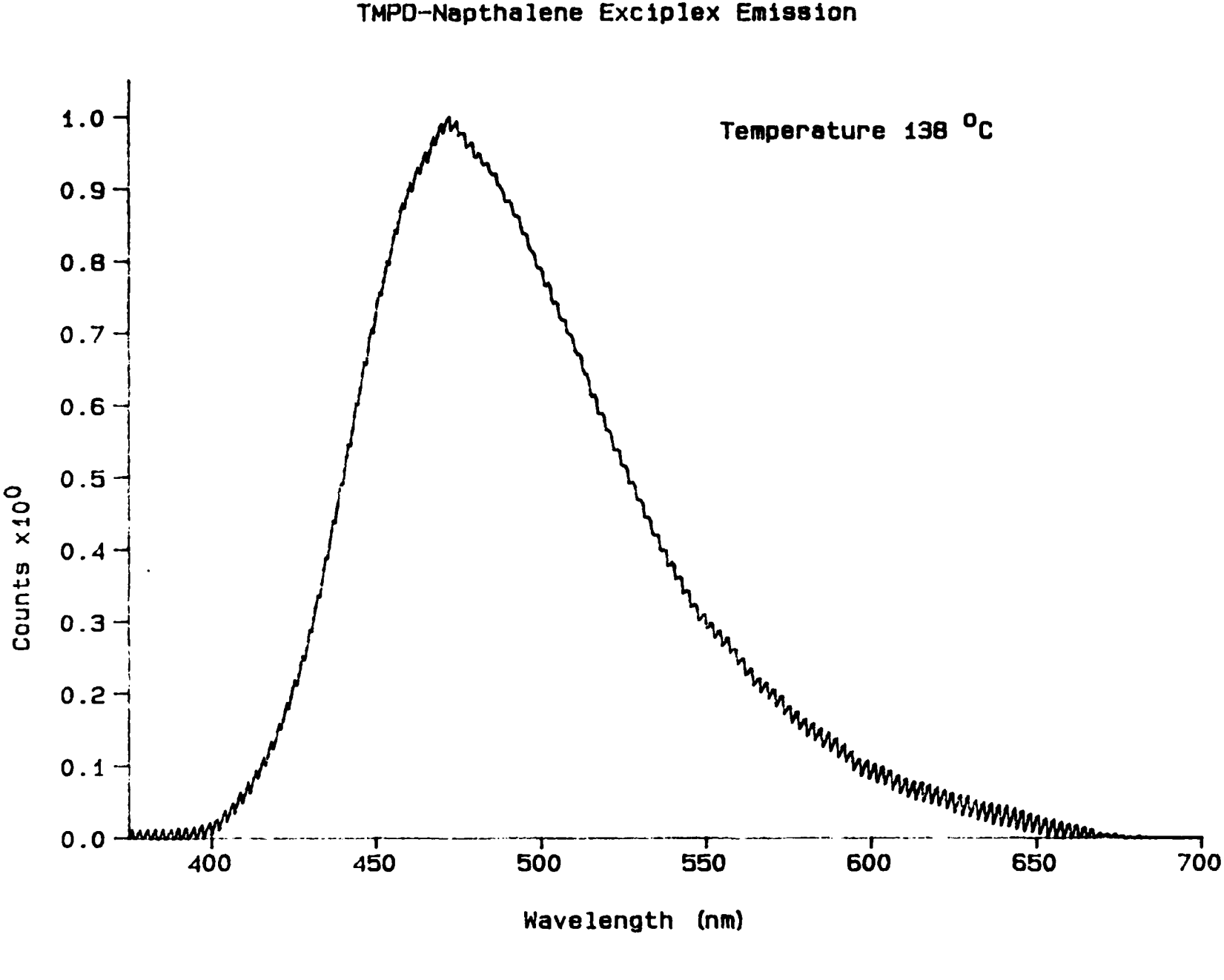
TMPD-Napthalene Exciplex Emission
Temperature 138 °C
Counts x10^0
1.0
0.9
0.8
0.7
0.6
0.5
0.4
0.3
0.2
0.1
0.0
400
450
500
550
600
650
700
Wavelength (nm)

SPECTRAL YIELD FUNCTION FOR SPECTRUM 5D

TMPD-Napthalene Exciplex

Wavelength	Intensity	Wavelength	Intensity	Wavelength	Intensity
396.0	7.570E-05	503.9	4.502E-03	611.8	4.526E-04
398.3	1.008E-04	506.2	4.346E-03	614.1	4.548E-04
400.7	1.381E-04	508.6	4.216E-03	616.5	4.228E-04
403.0	1.973E-04	510.9	4.058E-03	618.8	4.089E-04
405.4	2.549E-04	513.3	3.888E-03	621.2	3.848E-04
407.7	3.330E-04	515.6	3.720E-03	623.5	3.697E-04
410.1	4.224E-04	517.9	3.559E-03	625.8	3.399E-04
412.4	5.192E-04	520.3	3.407E-03	628.2	3.221E-04
414.7	6.258E-04	522.6	3.258E-03	630.5	2.922E-04
417.1	7.559E-04	525.0	3.119E-03	632.9	2.786E-04
419.4	8.968E-04	527.3	2.984E-03	635.2	2.664E-04
421.8	1.066E-03	529.7	2.829E-03	637.6	2.457E-04
424.1	1.260E-03	532.0	2.688E-03	639.9	2.372E-04
426.5	1.451E-03	534.4	2.543E-03	642.3	2.213E-04
428.8	1.660E-03	536.7	2.422E-03	644.6	2.128E-04
431.2	1.939E-03	539.1	2.312E-03	647.0	1.895E-04
433.5	2.248E-03	541.4	2.187E-03	649.3	1.681E-04
435.9	2.569E-03	543.7	2.074E-03	651.6	1.501E-04
438.2	2.884E-03	546.1	1.960E-03	654.0	1.328E-04
440.5	3.196E-03	548.4	1.872E-03	656.3	1.203E-04
442.9	3.534E-03	550.8	1.798E-03	658.7	1.044E-04
445.2	3.892E-03	553.1	1.737E-03	661.0	9.450E-05
447.6	4.192E-03	555.5	1.672E-03	663.4	7.371E-05
449.9	4.484E-03	557.8	1.594E-03	665.7	6.510E-05
452.3	4.752E-03	560.2	1.508E-03	668.1	3.600E-05
454.6	5.016E-03	562.5	1.423E-03	670.4	2.621E-05
457.0	5.260E-03	564.9	1.335E-03	672.8	2.450E-05
459.3	5.432E-03	567.2	1.296E-03	675.1	1.880E-05
461.7	5.579E-03	569.5	1.239E-03	677.4	1.341E-05
464.0	5.704E-03	571.9	1.184E-03	679.8	9.285E-06
466.3	5.823E-03	574.2	1.097E-03	682.1	3.713E-06
468.7	5.952E-03	576.6	1.050E-03	684.5	1.810E-06
471.0	6.031E-03	578.9	9.860E-04	686.8	1.547E-06
473.4	5.981E-03	581.3	9.488E-04	689.2	6.236E-06
475.7	5.908E-03	583.6	9.028E-04	691.5	1.421E-05
478.1	5.832E-03	586.0	8.525E-04	693.9	1.931E-05
480.4	5.744E-03	588.3	8.248E-04	696.2	3.354E-05
482.8	5.666E-03	590.7	7.650E-04	698.6	4.513E-05
485.1	5.568E-03	593.0	7.151E-04		
487.5	5.442E-03	595.4	6.575E-04		
489.8	5.352E-03	597.7	6.296E-04		
492.1	5.217E-03	600.0	6.057E-04		
494.5	5.066E-03	602.4	5.858E-04		
496.8	4.913E-03	604.7	5.592E-04		
499.2	4.783E-03	607.1	5.092E-04		
501.5	4.657E-03	609.4	4.902E-04		

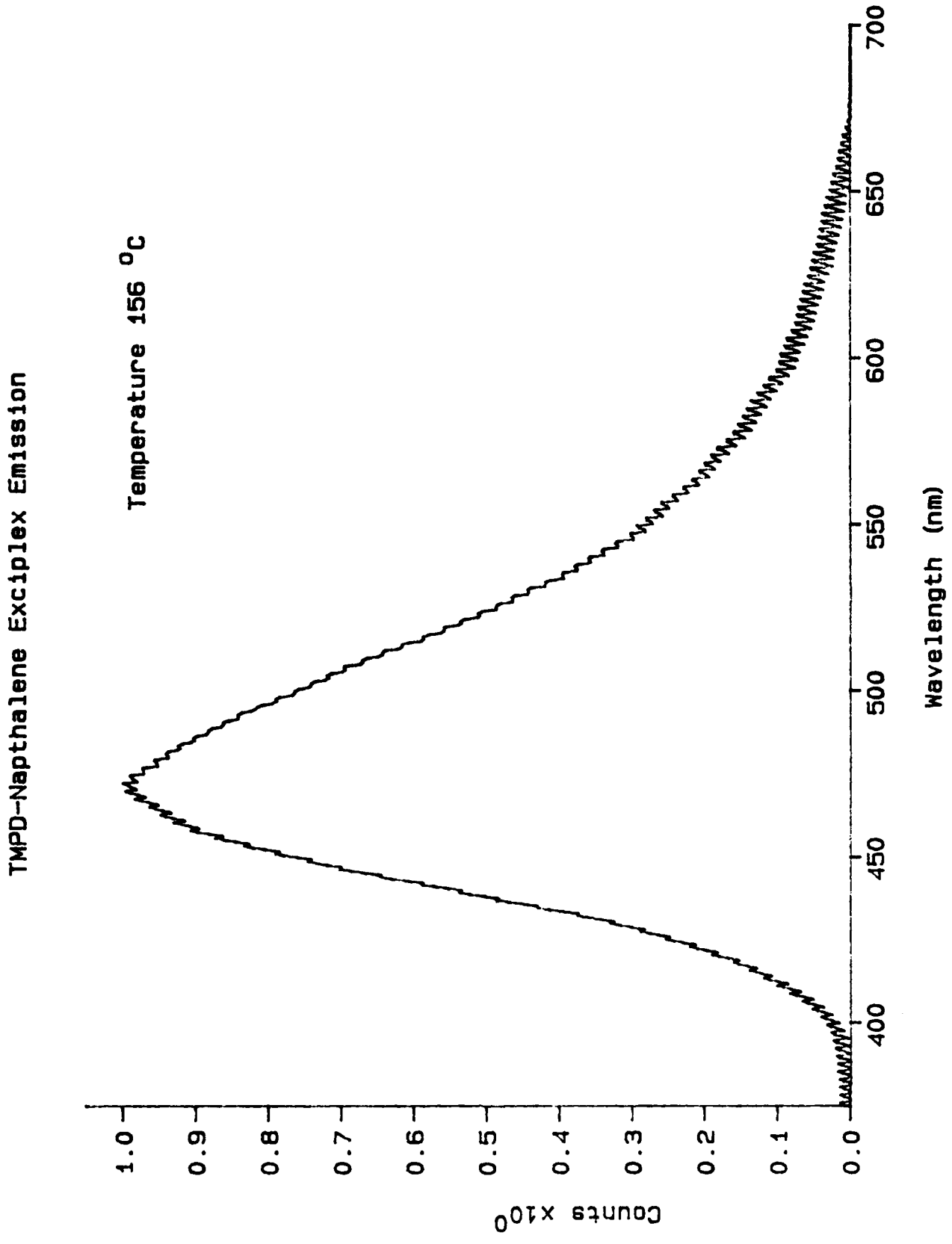
TMPD-Napthalene Exciplex Emission
Temperature 156 °C
Counts x10^0
1.0
0.9
0.8
0.7
0.6
0.5
0.4
0.3
0.2
0.1
0.0
400
450
500
550
600
650
700
Wavelength (nm)

SPECTRAL YIELD FUNCTION FOR SPECTRUM 5E

TMPD-Napthalene Exciplex

Wavelength	Intensity	Wavelength	Intensity	Wavelength	Intensity
395.4	7.521E-05	503.3	4.364E-03	611.2	3.530E-04
397.7	1.103E-04	505.6	4.223E-03	613.5	3.455E-04
400.1	1.503E-04	508.0	4.077E-03	615.9	3.145E-04
402.4	2.105E-04	510.3	3.915E-03	618.2	3.031E-04
404.8	2.896E-04	512.7	3.754E-03	620.6	2.863E-04
407.1	3.817E-04	515.0	3.567E-03	622.9	2.674E-04
409.5	4.874E-04	517.4	3.398E-03	625.3	2.390E-04
411.8	6.024E-04	519.7	3.259E-03	627.6	2.108E-04
414.2	7.339E-04	522.1	3.099E-03	629.9	1.970E-04
416.5	8.596E-04	524.4	2.958E-03	632.3	1.843E-04
418.8	1.020E-03	526.7	2.824E-03	634.6	1.635E-04
421.2	1.194E-03	529.1	2.689E-03	637.0	1.519E-04
423.5	1.396E-03	531.4	2.551E-03	639.3	1.378E-04
425.9	1.600E-03	533.8	2.408E-03	641.7	1.234E-04
428.2	1.829E-03	536.1	2.287E-03	644.0	1.113E-04
430.6	2.089E-03	538.5	2.181E-03	646.4	1.004E-04
432.9	2.396E-03	540.8	2.065E-03	648.7	8.290E-05
435.3	2.744E-03	543.2	1.942E-03	651.1	6.327E-05
437.6	3.059E-03	545.5	1.818E-03	653.4	4.800E-05
440.0	3.364E-03	547.9	1.720E-03	655.7	4.136E-05
442.3	3.709E-03	550.2	1.666E-03	658.1	2.203E-05
444.7	4.057E-03	552.5	1.592E-03	660.4	1.642E-05
447.0	4.377E-03	554.9	1.529E-03	662.8	5.013E-06
449.3	4.626E-03	557.2	1.461E-03	665.1	1.022E-06
451.7	4.895E-03	559.6	1.371E-03	667.5	3.760E-06
454.0	5.146E-03	561.9	1.286E-03	669.8	9.619E-06
456.4	5.364E-03	564.3	1.206E-03	672.2	2.322E-06
458.7	5.523E-03	566.6	1.160E-03	674.5	1.357E-05
461.1	5.657E-03	569.0	1.118E-03	676.9	1.741E-05
463.4	5.752E-03	571.3	1.051E-03	679.2	2.517E-05
465.8	5.863E-03	573.7	9.871E-04	681.5	4.613E-05
468.1	5.958E-03	576.0	9.193E-04	683.9	6.417E-05
470.5	6.022E-03	578.3	8.681E-04	686.2	6.836E-05
472.8	6.003E-03	580.7	8.250E-04	688.6	7.534E-05
475.1	5.921E-03	583.0	7.850E-04	690.9	8.377E-05
477.5	5.807E-03	585.4	7.366E-04	693.3	8.995E-05
479.8	5.709E-03	587.7	6.991E-04	695.6	1.013E-04
482.2	5.608E-03	590.1	6.522E-04	698.0	1.099E-04
484.5	5.487E-03	592.4	6.085E-04		
486.9	5.374E-03	594.8	5.517E-04		
489.2	5.244E-03	597.1	5.180E-04		
491.6	5.123E-03	599.5	4.941E-04		
493.9	4.981E-03	601.8	4.671E-04		
496.3	4.801E-03	604.1	4.485E-04		
498.6	4.652E-03	606.5	4.153E-04		
500.9	4.514E-03	608.8	3.722E-04		

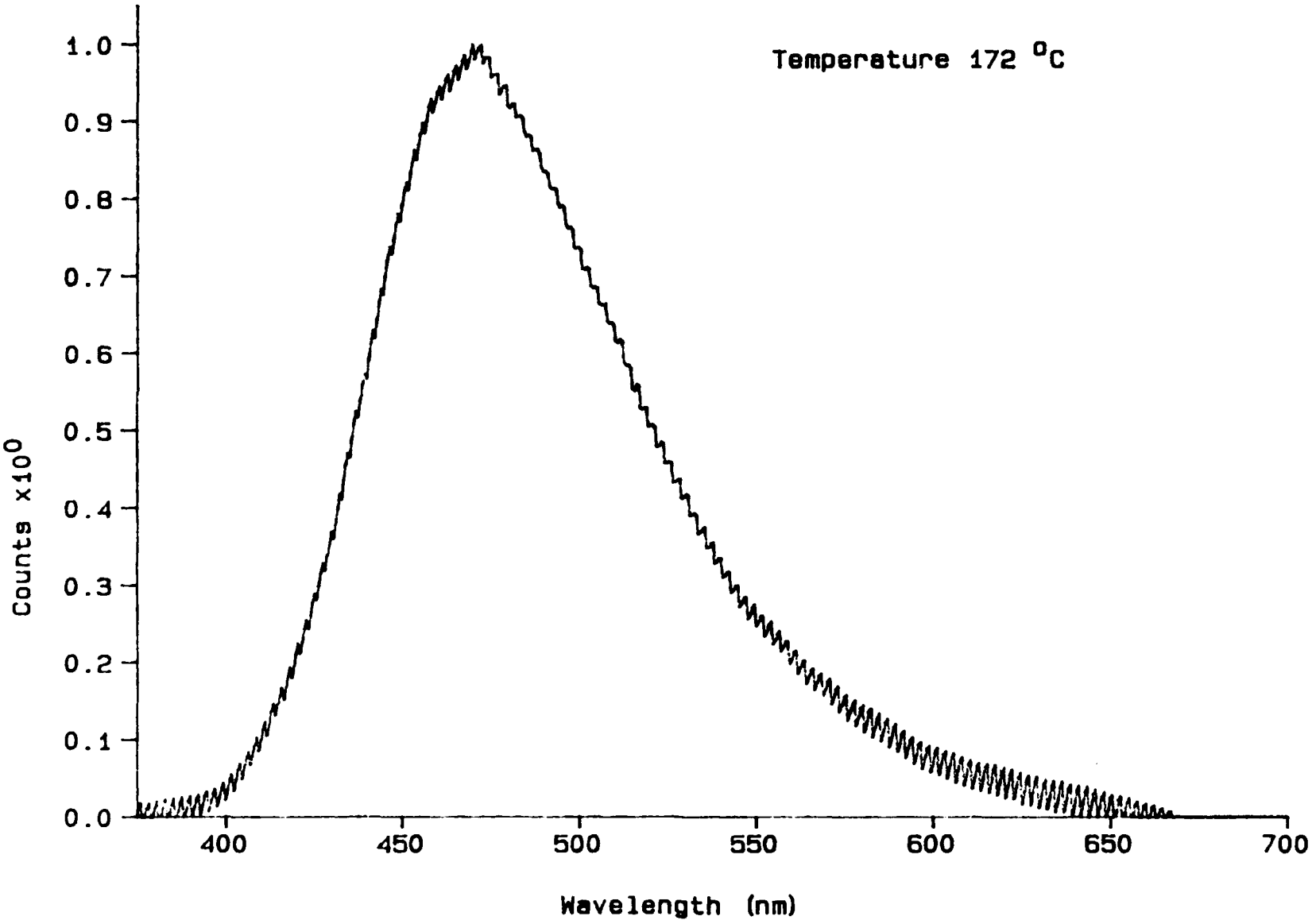
TMPD-Napthalene Exciplex Emission
Temperature 172 °C
Counts x10⁰
1.0
0.9
0.8
0.7
0.6
0.5
0.4
0.3
0.2
0.1
0.0
400
450
500
550
600
650
700
Wavelength (nm)

SPECTRAL YIELD FUNCTION FOR SPECTRUM 5F

TMPD-Napthalene Exciplex

Wavelength	Intensity	Wavelength	Intensity	Wavelength	Intensity
393.0	9.453E-05	500.9	4.365E-03	608.8	3.295E-04
395.4	1.180E-04	503.3	4.220E-03	611.2	3.069E-04
397.7	1.560E-04	505.6	4.082E-03	613.5	2.948E-04
400.1	2.142E-04	508.0	3.936E-03	615.9	2.737E-04
402.4	2.945E-04	510.3	3.781E-03	618.2	2.656E-04
404.8	3.868E-04	512.7	3.601E-03	620.6	2.428E-04
407.1	4.938E-04	515.0	3.396E-03	622.9	2.312E-04
409.5	6.132E-04	517.4	3.248E-03	625.3	1.962E-04
411.8	7.399E-04	519.7	3.124E-03	627.6	1.945E-04
414.2	8.984E-04	522.1	2.957E-03	629.9	1.660E-04
416.5	1.036E-03	524.4	2.824E-03	632.3	1.449E-04
418.8	1.213E-03	526.7	2.674E-03	634.6	1.280E-04
421.2	1.399E-03	529.1	2.552E-03	637.0	1.228E-04
423.5	1.607E-03	531.4	2.411E-03	639.3	1.023E-04
425.9	1.841E-03	533.8	2.273E-03	641.7	9.897E-05
428.2	2.075E-03	536.1	2.155E-03	644.0	8.266E-05
430.6	2.340E-03	538.5	2.038E-03	646.4	6.899E-05
432.9	2.678E-03	540.8	1.930E-03	648.7	5.091E-05
435.3	3.004E-03	543.2	1.810E-03	651.1	3.282E-05
437.6	3.322E-03	545.5	1.707E-03	653.4	1.915E-05
440.0	3.648E-03	547.9	1.618E-03	655.7	1.025E-05
442.3	3.959E-03	550.2	1.558E-03	658.1	4.945E-06
444.7	4.306E-03	552.5	1.484E-03	660.4	1.695E-05
447.0	4.606E-03	554.9	1.410E-03	662.8	2.629E-05
449.3	4.872E-03	557.2	1.364E-03	665.1	3.248E-05
451.7	5.127E-03	559.6	1.259E-03	667.5	3.819E-05
454.0	5.357E-03	561.9	1.188E-03	669.8	3.796E-05
456.4	5.550E-03	564.3	1.113E-03	672.2	5.438E-05
458.7	5.707E-03	566.6	1.067E-03	674.5	6.111E-05
461.1	5.809E-03	569.0	1.016E-03	676.9	6.333E-05
463.4	5.863E-03	571.3	9.604E-04	679.2	7.265E-05
465.8	5.963E-03	573.7	8.920E-04	681.5	8.766E-05
468.1	6.023E-03	576.0	8.332E-04	683.9	9.583E-05
470.5	6.103E-03	578.3	7.909E-04	686.2	9.918E-05
472.8	6.057E-03	580.7	7.507E-04	688.6	1.013E-04
475.1	5.924E-03	583.0	7.056E-04	690.9	1.091E-04
477.5	5.809E-03	585.4	6.762E-04	693.3	1.175E-04
479.8	5.653E-03	587.7	6.321E-04	695.6	1.310E-04
482.2	5.588E-03	590.1	5.836E-04	698.0	1.376E-04
484.5	5.426E-03	592.4	5.368E-04		
486.9	5.322E-03	594.8	4.887E-04		
489.2	5.148E-03	597.1	4.654E-04		
491.6	5.008E-03	599.5	4.327E-04		
493.9	4.860E-03	601.8	4.137E-04		
496.3	4.694E-03	604.1	3.937E-04		
498.6	4.535E-03	606.5	3.646E-04		

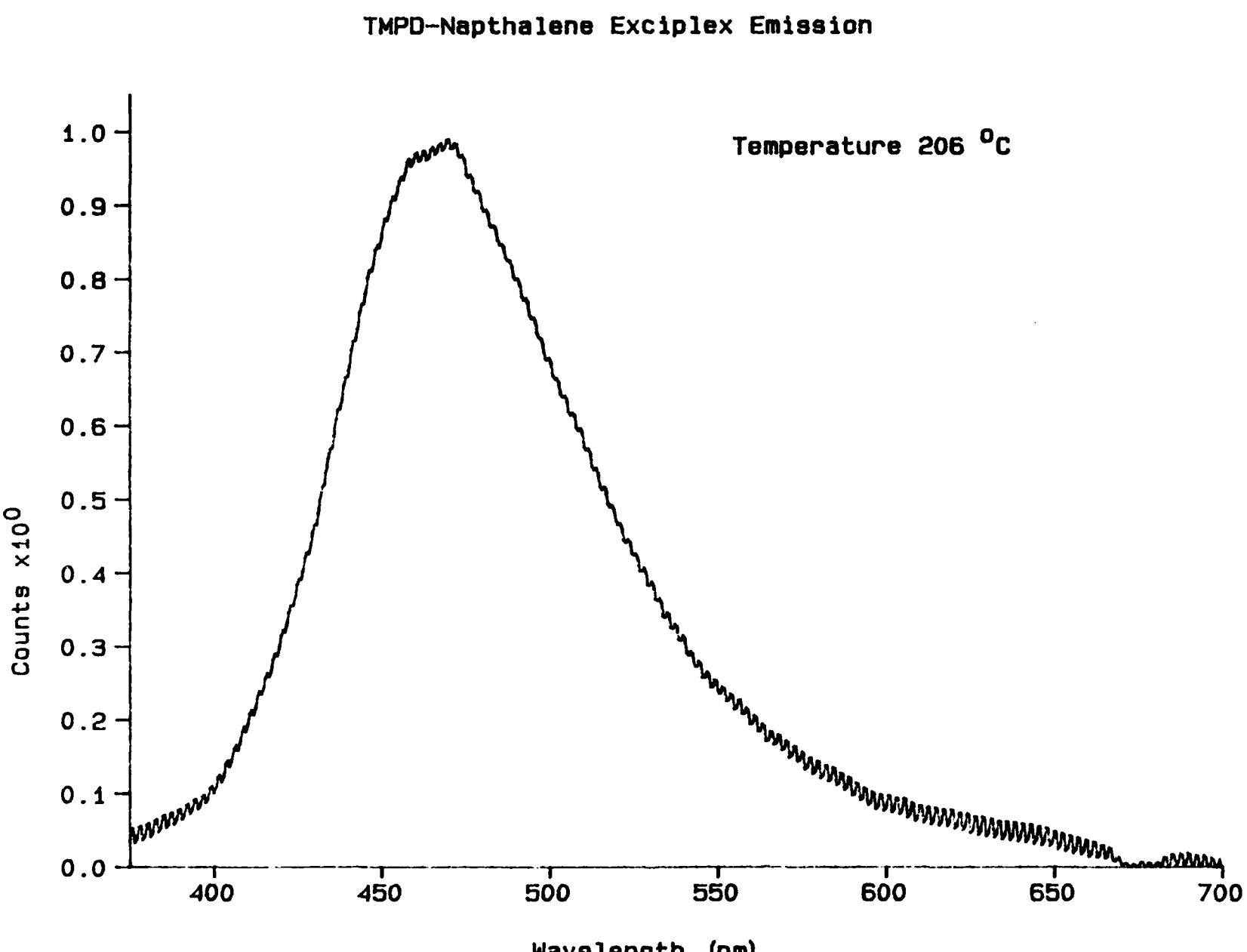
TMPD-Napthalene Exciplex Emission
Temperature 206 °C
Counts x10⁰
1.0
0.9
0.8
0.7
0.6
0.5
0.4
0.3
0.2
0.1
0.0
400
450
500
550
600
650
700
Wavelength (nm)

SPECTRAL YIELD FUNCTION FOR SPECTRUM 5G

TMPD-Napthalene Exciplex

Wavelength	Intensity	Wavelength	Intensity	Wavelength	Intensity
376.6	2.274E-04	484.5	4.941E-03	592.4	5.530E-04
379.0	2.466E-04	486.9	4.815E-03	594.8	5.173E-04
381.3	2.765E-04	489.2	4.666E-03	597.1	4.888E-04
383.7	3.148E-04	491.6	4.505E-03	599.5	4.767E-04
386.0	3.452E-04	493.9	4.354E-03	601.8	4.630E-04
388.4	3.720E-04	496.3	4.207E-03	604.1	4.551E-04
390.7	4.137E-04	498.6	4.023E-03	606.5	4.240E-04
393.0	4.554E-04	500.9	3.871E-03	608.8	3.954E-04
395.4	4.862E-04	503.3	3.731E-03	611.2	3.824E-04
397.7	5.467E-04	505.6	3.592E-03	613.5	3.783E-04
400.1	6.263E-04	508.0	3.465E-03	615.9	3.640E-04
402.4	7.250E-04	510.3	3.309E-03	618.2	3.596E-04
404.8	8.473E-04	512.7	3.151E-03	620.6	3.371E-04
407.1	9.809E-04	515.0	2.997E-03	622.9	3.291E-04
409.5	1.128E-03	517.4	2.857E-03	625.3	3.035E-04
411.8	1.260E-03	519.7	2.719E-03	627.6	2.959E-04
414.2	1.416E-03	522.1	2.577E-03	629.9	2.820E-04
416.5	1.560E-03	524.4	2.475E-03	632.3	2.681E-04
418.8	1.734E-03	526.7	2.347E-03	634.6	2.573E-04
421.2	1.923E-03	529.1	2.235E-03	637.0	2.505E-04
423.5	2.141E-03	531.4	2.111E-03	639.3	2.398E-04
425.9	2.349E-03	533.8	1.980E-03	641.7	2.340E-04
428.2	2.549E-03	536.1	1.893E-03	644.0	2.193E-04
430.6	2.807E-03	538.5	1.799E-03	646.4	2.110E-04
432.9	3.123E-03	540.8	1.681E-03	648.7	1.940E-04
435.3	3.419E-03	543.2	1.591E-03	651.1	1.742E-04
437.6	3.708E-03	545.5	1.504E-03	653.4	1.575E-04
440.0	3.988E-03	547.9	1.432E-03	655.7	1.467E-04
442.3	4.274E-03	550.2	1.382E-03	658.1	1.336E-04
444.7	4.561E-03	552.5	1.325E-03	660.4	1.156E-04
447.0	4.799E-03	554.9	1.263E-03	662.8	9.761E-05
449.3	4.986E-03	557.2	1.218E-03	665.1	8.742E-05
451.7	5.196E-03	559.6	1.141E-03	667.5	4.462E-05
454.0	5.351E-03	561.9	1.080E-03	669.8	1.509E-05
456.4	5.513E-03	564.3	1.009E-03	672.2	3.006E-06
458.7	5.597E-03	566.6	9.852E-04	674.5	8.846E-06
461.1	5.626E-03	569.0	9.403E-04	676.9	6.144E-06
463.4	5.636E-03	571.3	8.881E-04	679.2	3.819E-06
465.8	5.678E-03	573.7	8.545E-04	681.5	2.056E-05
468.1	5.718E-03	576.0	7.950E-04	683.9	3.138E-05
470.5	5.710E-03	578.3	7.640E-04	686.2	3.884E-05
472.8	5.636E-03	580.7	7.294E-04	688.6	3.771E-05
475.1	5.475E-03	583.0	7.089E-04	690.9	2.850E-05
477.5	5.351E-03	585.4	6.708E-04	693.3	2.236E-05
479.8	5.205E-03	587.7	6.353E-04	695.6	4.546E-06
482.2	5.079E-03	590.1	5.884E-04	698.0	5.362E-06

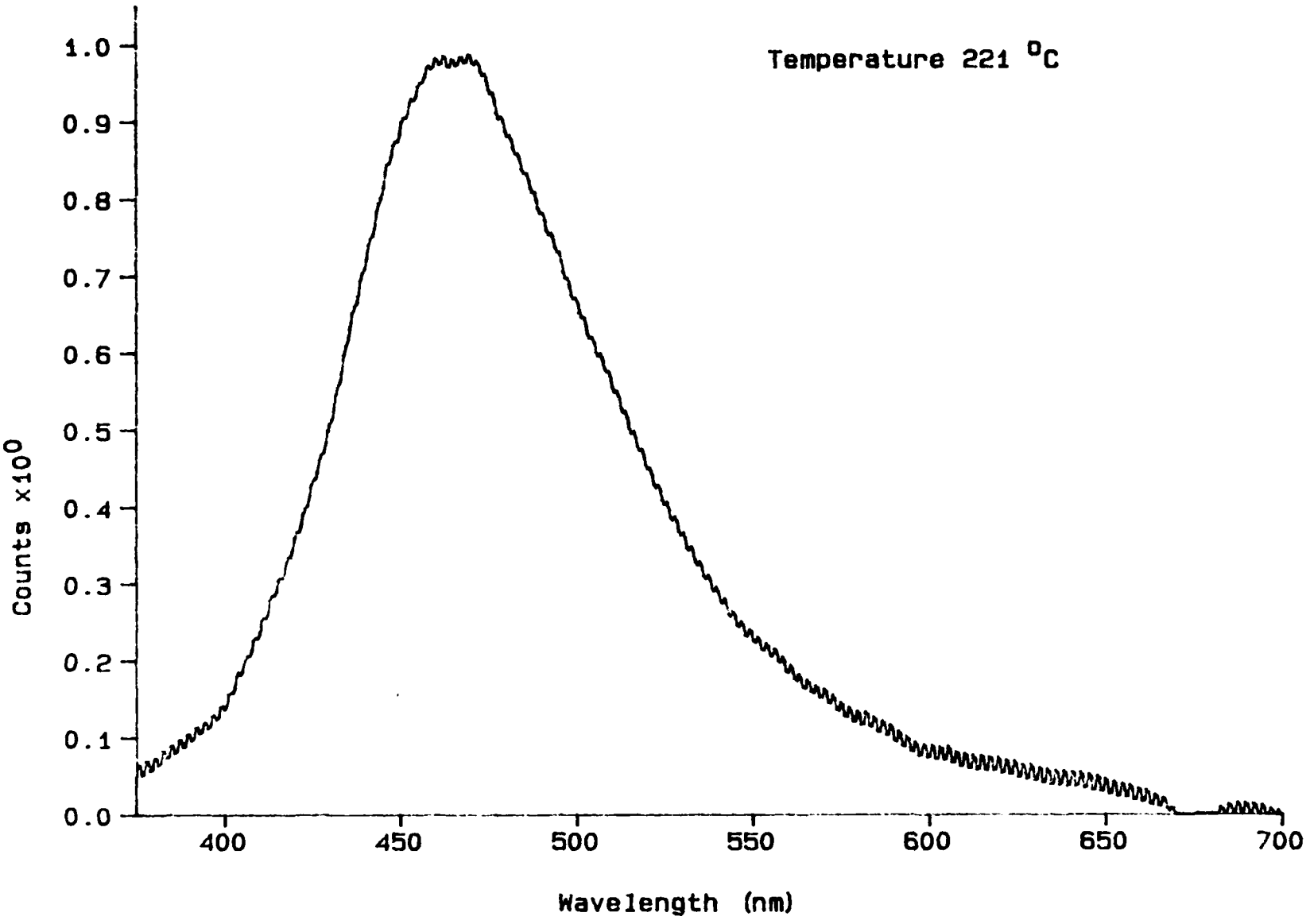
TMPD-Napthalene Exciplex Emission
Temperature 221 °C
Counts x10^0
1.0
0.9
0.8
0.7
0.6
0.5
0.4
0.3
0.2
0.1
0.0
400
450
500
550
600
650
700
Wavelength (nm)

SPECTRAL YIELD FUNCTION FOR SPECTRUM 5H

TMPD-Napthalene Exciplex

Wavelength	Intensity	Wavelength	Intensity	Wavelength	Intensity
371.9	2.331E-04	479.8	5.080E-03	587.7	5.896E-04
374.3	2.728E-04	482.2	4.949E-03	590.1	5.420E-04
376.6	3.044E-04	484.5	4.801E-03	592.4	5.069E-04
379.0	3.332E-04	486.9	4.660E-03	594.8	4.712E-04
381.3	3.890E-04	489.2	4.502E-03	597.1	4.436E-04
383.7	4.306E-04	491.6	4.342E-03	599.5	4.332E-04
386.0	4.704E-04	493.9	4.210E-03	601.8	4.187E-04
388.4	5.120E-04	496.3	4.018E-03	604.1	4.121E-04
390.7	5.669E-04	498.6	3.859E-03	606.5	3.851E-04
393.0	6.165E-04	500.9	3.718E-03	608.8	3.626E-04
395.4	6.563E-04	503.3	3.562E-03	611.2	3.482E-04
397.7	7.286E-04	505.6	3.432E-03	613.5	3.429E-04
400.1	8.118E-04	508.0	3.312E-03	615.9	3.335E-04
402.4	9.446E-04	510.3	3.159E-03	618.2	3.340E-04
404.8	1.074E-03	512.7	3.010E-03	620.6	3.151E-04
407.1	1.220E-03	515.0	2.852E-03	622.9	3.025E-04
409.5	1.357E-03	517.4	2.721E-03	625.3	2.783E-04
411.8	1.509E-03	519.7	2.583E-03	627.6	2.702E-04
414.2	1.671E-03	522.1	2.442E-03	629.9	2.577E-04
416.5	1.807E-03	524.4	2.320E-03	632.3	2.423E-04
418.8	1.975E-03	526.7	2.200E-03	634.6	2.312E-04
421.2	2.157E-03	529.1	2.088E-03	637.0	2.270E-04
423.5	2.370E-03	531.4	1.976E-03	639.3	2.162E-04
425.9	2.586E-03	533.8	1.864E-03	641.7	2.142E-04
428.2	2.763E-03	536.1	1.761E-03	644.0	1.987E-04
430.6	3.023E-03	538.5	1.669E-03	646.4	1.849E-04
432.9	3.316E-03	540.8	1.580E-03	648.7	1.749E-04
435.3	3.636E-03	543.2	1.480E-03	651.1	1.554E-04
437.6	3.890E-03	545.5	1.401E-03	653.4	1.401E-04
440.0	4.157E-03	547.9	1.330E-03	655.7	1.330E-04
442.3	4.402E-03	550.2	1.284E-03	658.1	1.125E-04
444.7	4.695E-03	552.5	1.224E-03	660.4	9.897E-05
447.0	4.924E-03	554.9	1.180E-03	662.8	7.856E-05
449.3	5.088E-03	557.2	1.134E-03	665.1	6.331E-05
451.7	5.253E-03	559.6	1.058E-03	667.5	2.201E-05
454.0	5.377E-03	561.9	9.993E-04	669.8	1.519E-05
456.4	5.518E-03	564.3	9.435E-04	672.2	2.852E-05
458.7	5.603E-03	566.6	9.051E-04	674.5	1.748E-05
461.1	5.628E-03	569.0	8.705E-04	676.9	2.343E-05
463.4	5.603E-03	571.3	8.285E-04	679.2	2.493E-05
465.8	5.621E-03	573.7	7.718E-04	681.5	2.039E-06
468.1	5.641E-03	576.0	7.269E-04	683.9	8.575E-06
470.5	5.620E-03	578.3	6.920E-04	686.2	1.638E-05
472.8	5.535E-03	580.7	6.746E-04	688.6	1.637E-05
475.1	5.400E-03	583.0	6.555E-04	690.9	7.454E-06
477.5	5.211E-03	585.4	6.181E-04	693.3	8.479E-07

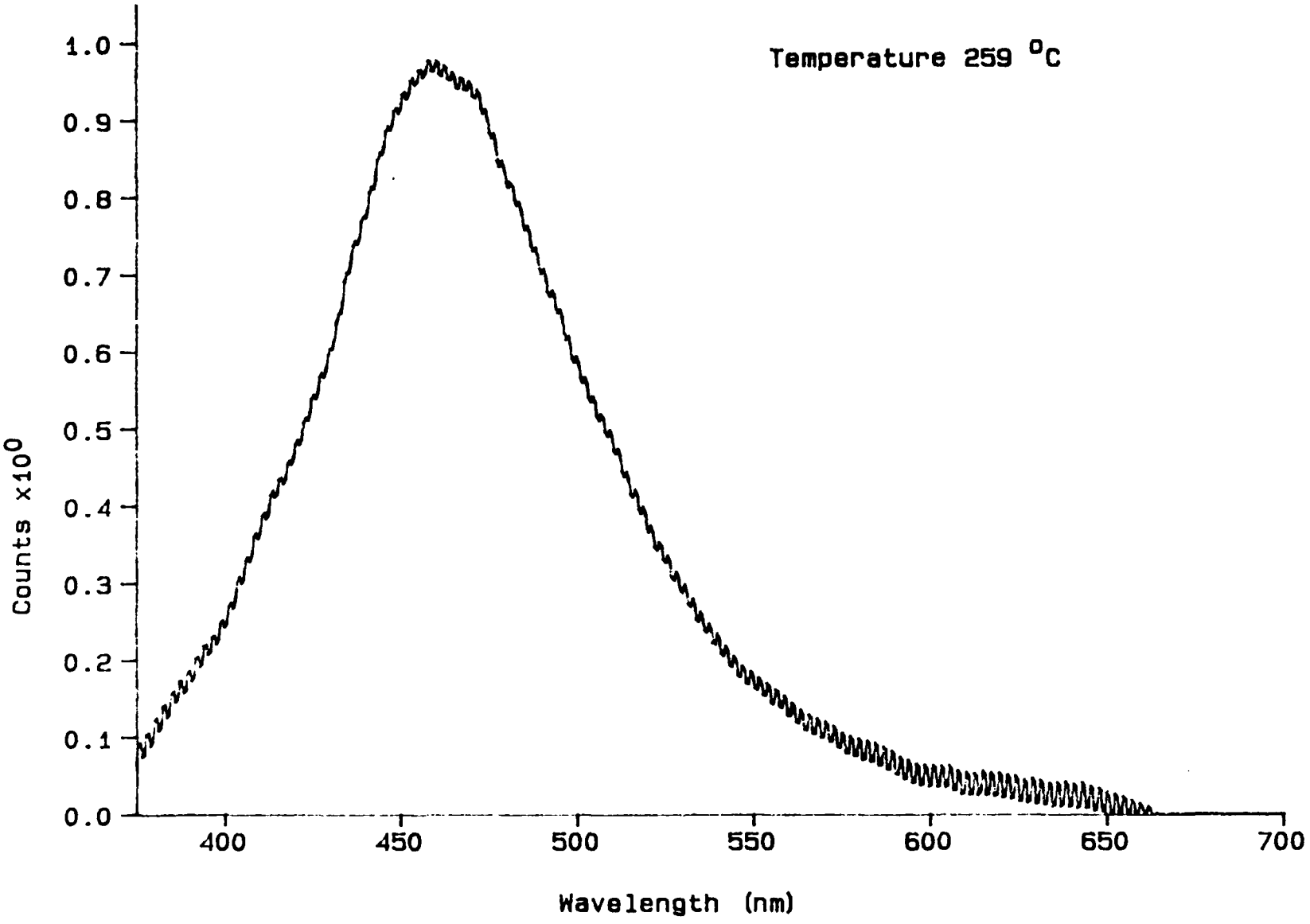
TMPD-Napthalene Exciplex Emission
Temperature 259 °C
Counts x10⁰
1.0
0.9
0.8
0.7
0.6
0.5
0.4
0.3
0.2
0.1
0.0
400
450
500
550
600
650
700
Wavelength (nm)

SPECTRAL YIELD FUNCTION FOR SPECTRUM 51

TMPD-Napthalene Exciplex

Wavelength	Intensity	Wavelength	Intensity	Wavelength	Intensity
371.9	2.700E-04	479.8	4.833E-03	587.7	3.466E-04
374.3	3.807E-04	482.2	4.691E-03	590.1	3.061E-04
376.6	4.655E-04	484.5	4.503E-03	592.4	2.761E-04
379.0	5.601E-04	486.9	4.340E-03	594.8	2.462E-04
381.3	6.774E-04	489.2	4.167E-03	597.1	2.331E-04
383.7	7.774E-04	491.6	3.991E-03	599.5	2.272E-04
386.0	8.878E-04	493.9	3.880E-03	601.8	2.172E-04
388.4	9.614E-04	496.3	3.656E-03	604.1	2.187E-04
390.7	1.063E-03	498.6	3.483E-03	606.5	1.867E-04
393.0	1.162E-03	500.9	3.327E-03	608.8	1.641E-04
395.4	1.252E-03	503.3	3.176E-03	611.2	1.566E-04
397.7	1.345E-03	505.6	3.034E-03	613.5	1.710E-04
400.1	1.480E-03	508.0	2.915E-03	615.9	1.544E-04
402.4	1.655E-03	510.3	2.776E-03	618.2	1.532E-04
404.8	1.818E-03	512.7	2.602E-03	620.6	1.393E-04
407.1	2.005E-03	515.0	2.443E-03	622.9	1.284E-04
409.5	2.171E-03	517.4	2.318E-03	625.3	1.028E-04
411.8	2.323E-03	519.7	2.176E-03	627.6	1.066E-04
414.2	2.472E-03	522.1	2.032E-03	629.9	9.008E-05
416.5	2.579E-03	524.4	1.940E-03	632.3	8.072E-05
418.8	2.746E-03	526.7	1.804E-03	634.6	7.118E-05
421.2	2.897E-03	529.1	1.715E-03	637.0	7.625E-05
423.5	3.089E-03	531.4	1.602E-03	639.3	6.714E-05
425.9	3.250E-03	533.8	1.487E-03	641.7	6.526E-05
428.2	3.419E-03	536.1	1.401E-03	644.0	5.404E-05
430.6	3.652E-03	538.5	1.311E-03	646.4	3.170E-05
432.9	3.949E-03	540.8	1.222E-03	648.7	1.645E-05
435.3	4.248E-03	543.2	1.137E-03	651.1	6.807E-07
437.6	4.447E-03	545.5	1.058E-03	653.4	2.103E-05
440.0	4.657E-03	547.9	1.005E-03	655.7	2.987E-05
442.3	4.891E-03	550.2	9.592E-04	658.1	5.189E-05
444.7	5.136E-03	552.5	9.117E-04	660.4	7.391E-05
447.0	5.313E-03	554.9	8.516E-04	662.8	1.098E-04
449.3	5.437E-03	557.2	8.206E-04	665.1	1.471E-04
451.7	5.546E-03	559.6	7.571E-04	667.5	2.422E-04
454.0	5.645E-03	561.9	7.031E-04	669.8	3.372E-04
456.4	5.710E-03	564.3	6.512E-04	672.2	3.398E-04
458.7	5.734E-03	566.6	6.203E-04	674.5	2.994E-04
461.1	5.696E-03	569.0	5.955E-04	676.9	3.113E-04
463.4	5.658E-03	571.3	5.590E-04	679.2	3.052E-04
465.8	5.595E-03	573.7	5.110E-04	681.5	2.419E-04
468.1	5.581E-03	576.0	4.714E-04	683.9	2.039E-04
470.5	5.518E-03	578.3	4.531E-04	686.2	1.764E-04
472.8	5.400E-03	580.7	4.321E-04	688.6	1.690E-04
475.1	5.213E-03	583.0	4.154E-04	690.9	1.752E-04
477.5	4.989E-03	585.4	3.836E-04	693.3	1.840E-04

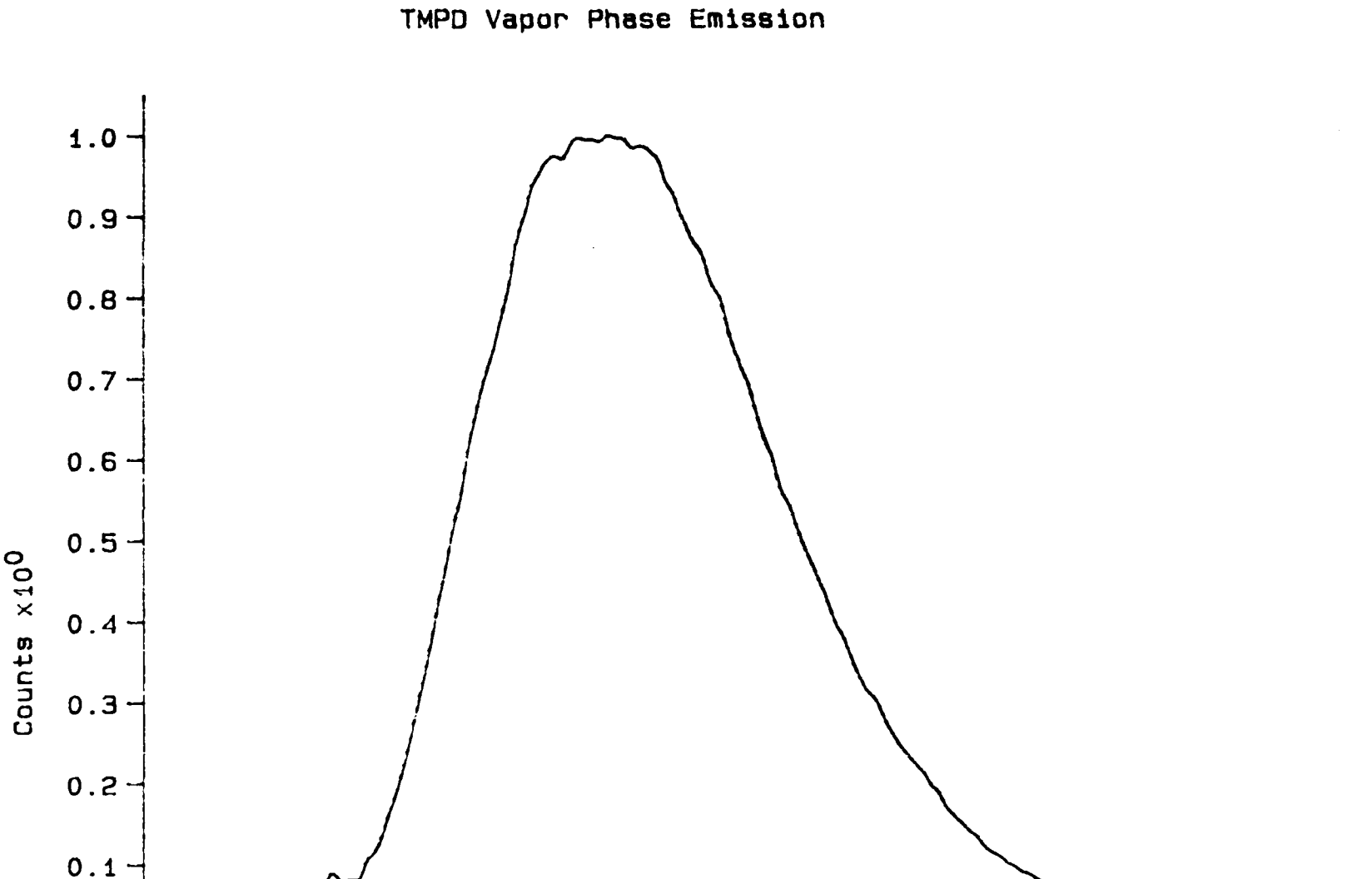
TMPD Vapor Phase Emission
1.0
0.9
0.8
0.7
0.6
0.5
0.4
0.3
0.2
0.1
0.0
Counts x10^0
300
320
340
360
380
400
420
440
460
480
500
520
Wavelength (nm)

SPECTRAL YIELD FUNCTION FOR SPECTRUM 6

TMPD Vapor

Wavelength	Intensity	Wavelength	Intensity	Wavelength	Intensity
327.8	2.587E-04	408.1	6.020E-03	488.4	2.518E-04
329.5	3.492E-04	409.8	5.781E-03	490.1	2.264E-04
331.2	5.132E-04	411.6	5.424E-03	491.9	2.009E-04
333.0	6.818E-04	413.3	5.145E-03	493.6	2.106E-04
334.7	7.077E-04	415.1	4.833E-03	495.4	1.953E-04
336.5	6.684E-04	416.8	4.584E-03	497.1	1.875E-04
340.0	8.417E-04	420.3	4.072E-03		
341.7	9.706E-04	422.0	3.849E-03		
343.5	1.201E-03	423.8	3.621E-03		
345.2	1.496E-03	425.5	3.344E-03		
347.0	1.853E-03	427.3	3.156E-03		
348.7	2.279E-03	429.0	2.897E-03		
350.5	2.707E-03	430.8	2.684E-03		
352.2	3.202E-03	432.5	2.558E-03		
353.9	3.717E-03	434.3	2.377E-03		
355.7	4.233E-03	436.0	2.186E-03		
357.4	4.652E-03	437.8	2.035E-03		
359.2	5.249E-03	439.5	1.918E-03		
360.9	5.676E-03	441.3	1.810E-03		
362.7	6.008E-03	443.0	1.665E-03		
364.4	6.395E-03	444.7	1.566E-03		
366.2	6.793E-03	446.5	1.387E-03		
367.9	7.349E-03	448.2	1.286E-03		
369.7	7.692E-03	450.0	1.190E-03		
371.4	7.921E-03	451.7	1.113E-03		
373.2	8.081E-03	453.5	9.984E-04		
374.9	8.105E-03	455.2	9.380E-04		
376.6	8.159E-03	457.0	8.662E-04		
378.4	8.302E-03	458.7	8.092E-04		
380.1	8.280E-03	460.5	7.526E-04		
381.9	8.271E-03	462.2	6.996E-04		
383.6	8.318E-03	464.0	6.488E-04		
385.4	8.301E-03	465.7	6.002E-04		
387.1	8.288E-03	467.4	5.672E-04		
388.9	8.204E-03	469.2	5.148E-04		
390.6	8.214E-03	470.9	4.815E-04		
392.4	8.135E-03	472.7	4.388E-04		
394.1	7.946E-03	474.4	4.232E-04		
395.9	7.747E-03	476.2	4.012E-04		
397.6	7.497E-03	477.9	3.490E-04		
399.3	7.274E-03	479.7	3.251E-04		
401.1	7.138E-03	481.4	3.348E-04		
402.8	6.846E-03	483.2	2.814E-04		
404.6	6.671E-03	484.9	2.744E-04		
406.3	6.303E-03	486.7	2.696E-04		

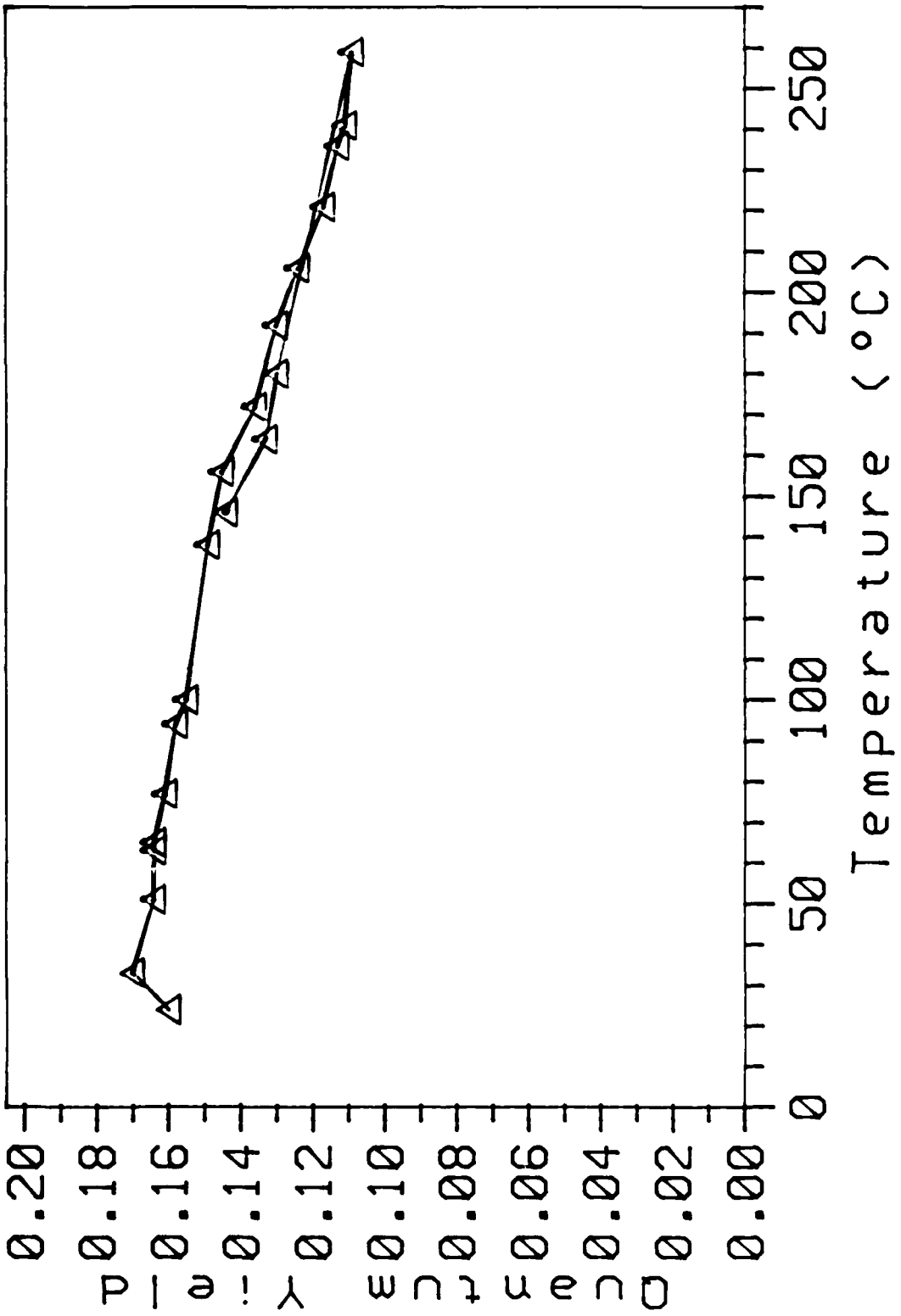
Quantum Yield
0.00
0.02
0.04
0.06
0.08
0.10
0.12
0.14
0.16
0.18
0.20
0
50
100
150
200
250
Temperature (°C)

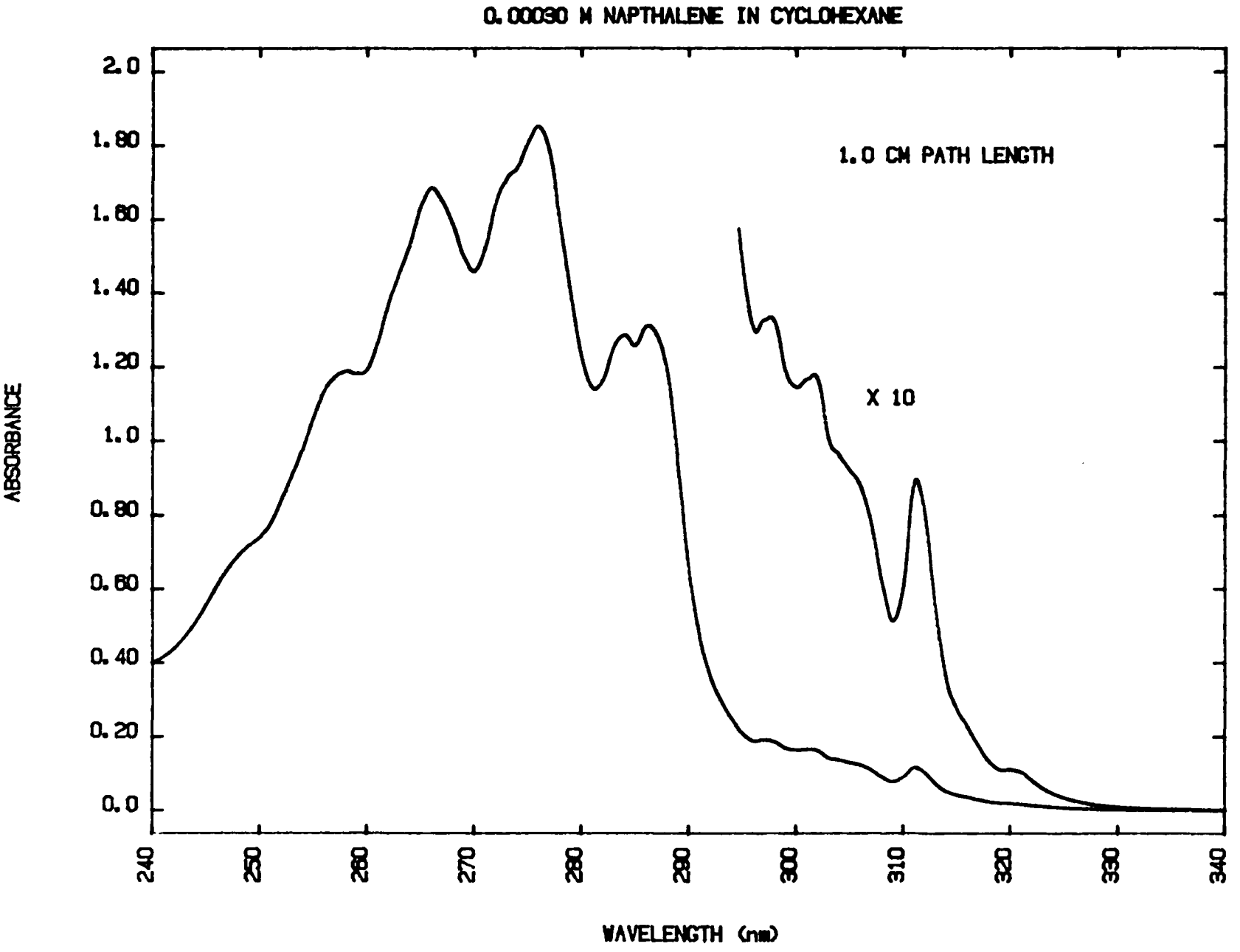
0.00030 M NAPTHALENE IN CYCLOHEXANE
1.0 CM PATH LENGTH
X 10
ABSORBANCE
2.0
1.80
1.60
1.40
1.20
1.0
0.80
0.60
0.40
0.20
0.0
240
250
260
270
280
290
300
310
320
330
340
WAVELENGTH (nm)

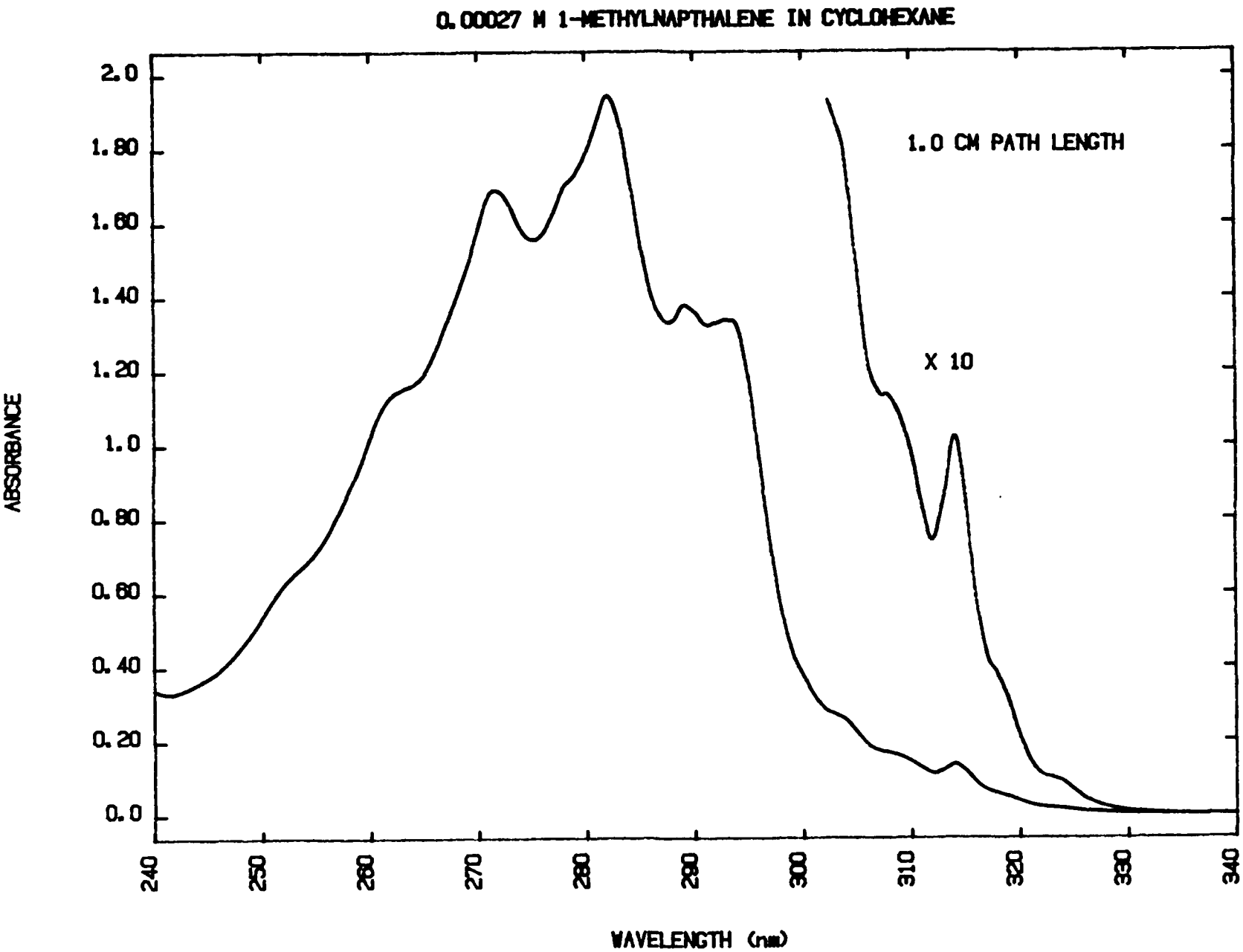
0.00027 M 1-METHYLNAPTHALENE IN CYCLOHEXANE
1.0 CM PATH LENGTH
X 10
ABSORBANCE
2.0
1.80
1.60
1.40
1.20
1.0
0.80
0.60
0.40
0.20
0.0
240
250
260
270
280
290
300
310
320
330
340
WAVELENGTH (nm)

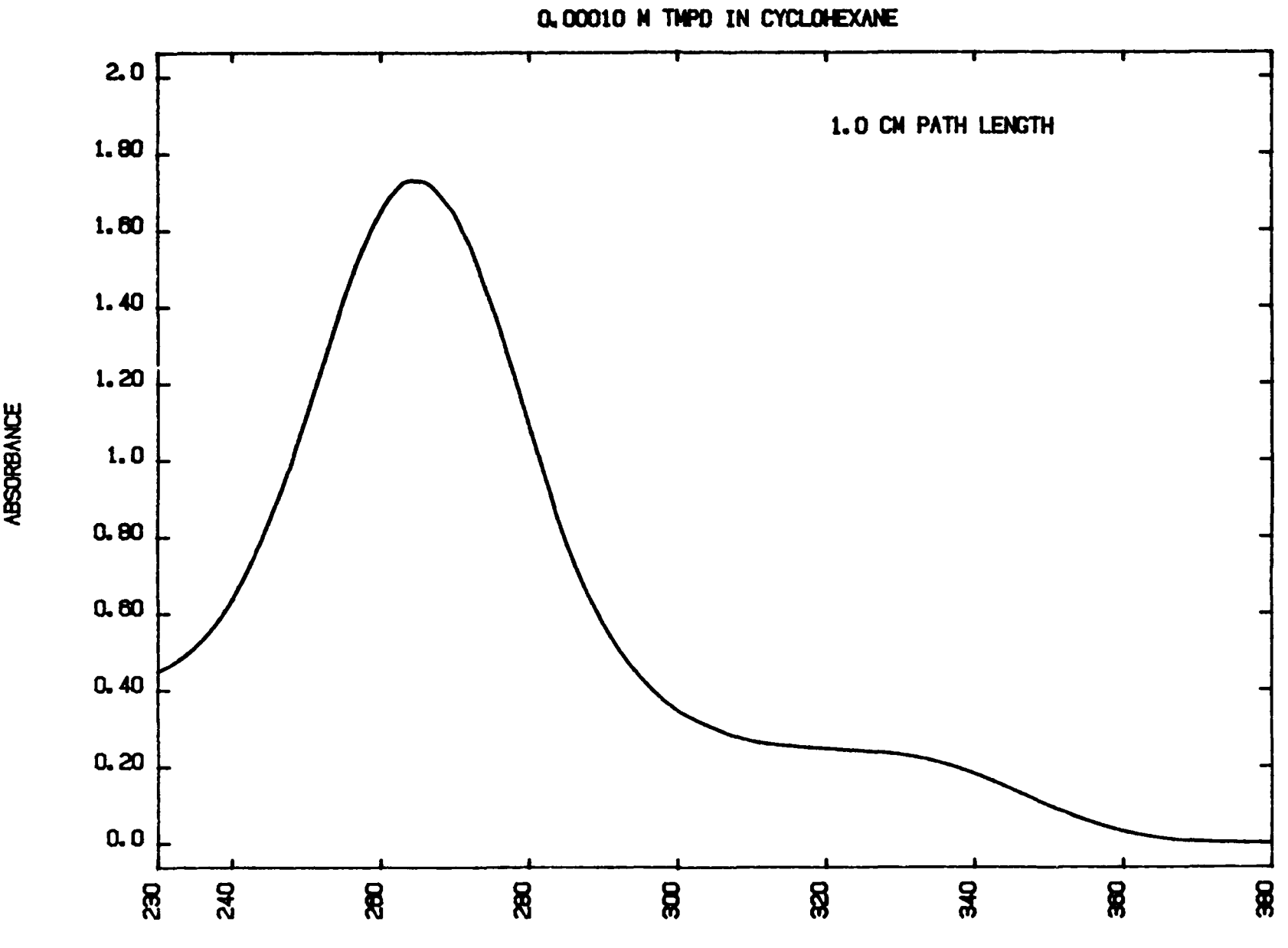
0.00010 M TMPD IN CYCLOHEXANE
1.0 CM PATH LENGTH
ABSORBANCE
2.0
1.80
1.60
1.40
1.20
1.0
0.80
0.60
0.40
0.20
0.0
230
240
260
280
300
320
340
360
380
WAVELENGTH (nm)

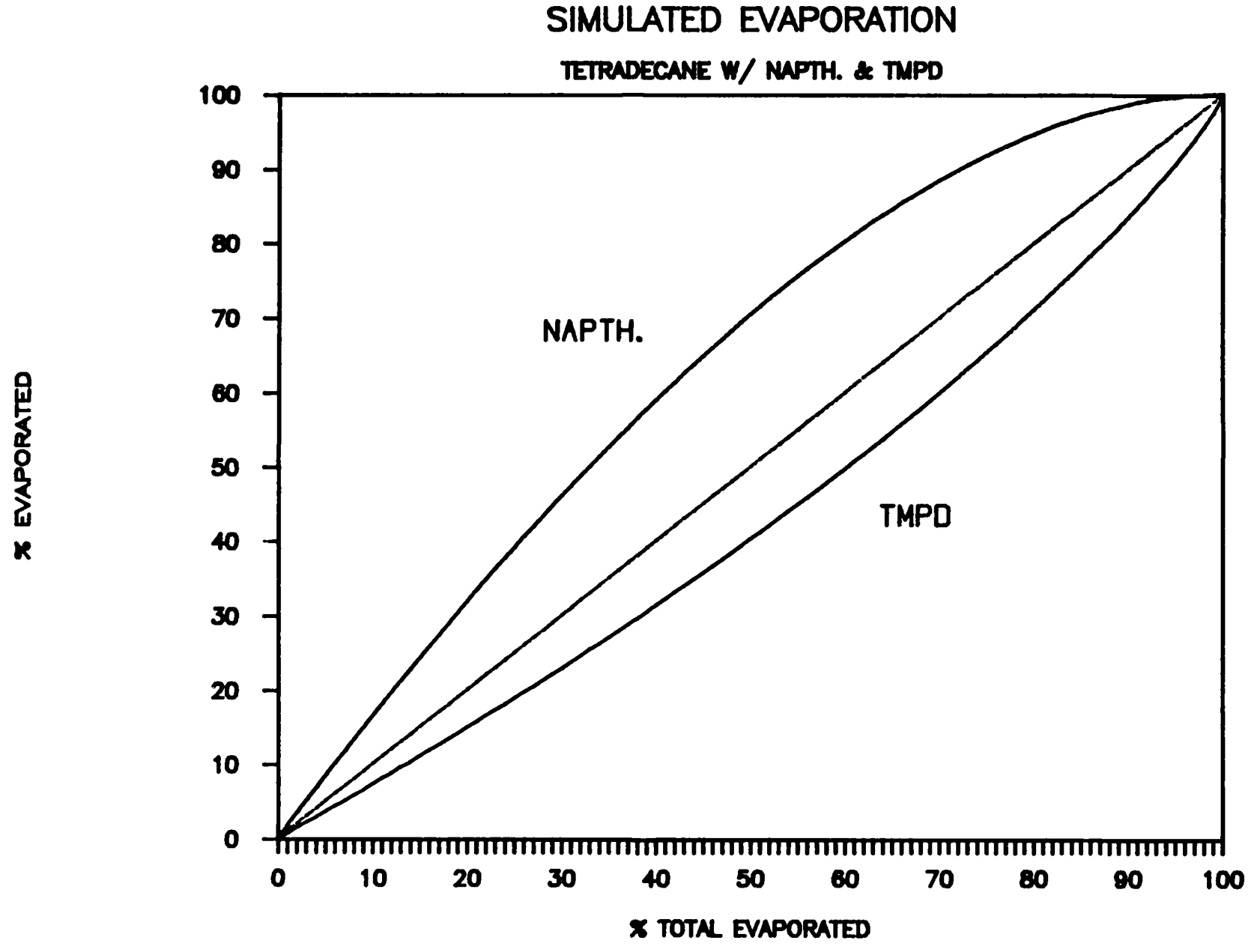
SIMULATED EVAPORATION
TETRADECANE W/ NAPTH. & TMPD
NAPTH.
TMPD
% EVAPORATED
% TOTAL EVAPORATED
0
10
20
30
40
50
60
70
80
90
100

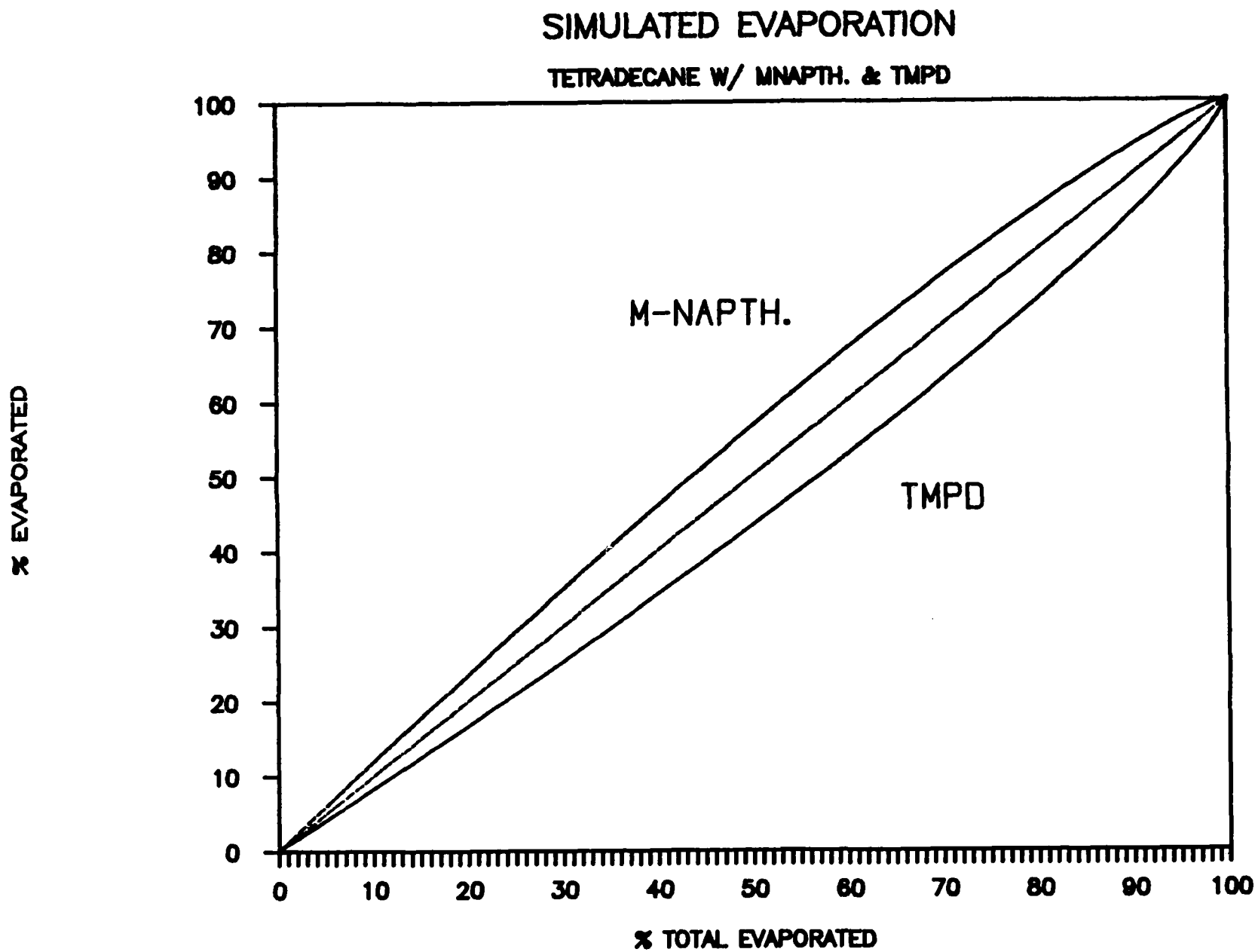
SIMULATED EVAPORATION
TETRADECANE W/ MNAPTH. & TMPD
M-NAPTH.
TMPD
% EVAPORATED
% TOTAL EVAPORATED
0
10
20
30
40
50
60
70
80
90
100

List of Publications

1. H. E. Gossage and L. A. Melton, "Fluorescence Thermometers Using Intramolecular Exciplexes," Appl. Opt., 26, 2256 (1987).

Scientific Personnel Employed

1. Dr. Alice M. Murray, postdoctoral scientist

2. Dr. Thomas D. Padrick, postdoctoral scientist

3. Mr. Stanley K. Nickle, graduate student, Doctor of Chemistry Program

END

DATE

FILMED

5-88

DTIC